

STATE OF WASHINGTON
Daniel J. Evans, Governor

DEPARTMENT OF ECOLOGY
JOHN A. BIGGS, Director

WATER-SUPPLY BULLETIN 44

**Digital Simulation of a Basalt Aquifer System,
Walla Walla River Basin, Washington and Oregon**

By
R. D. MAC NISH AND R. A. BARKER
of the
United States Geological Survey

Prepared Cooperatively by the
UNITED STATES GEOLOGICAL SURVEY

— 1976 —

STATE OF WASHINGTON
Daniel J. Evans, Governor

DEPARTMENT OF ECOLOGY
John A. Biggs, Director

Water-Supply Bulletin 44

DIGITAL SIMULATION OF A BASALT AQUIFER SYSTEM,
WALLA WALLA RIVER BASIN, WASHINGTON AND OREGON

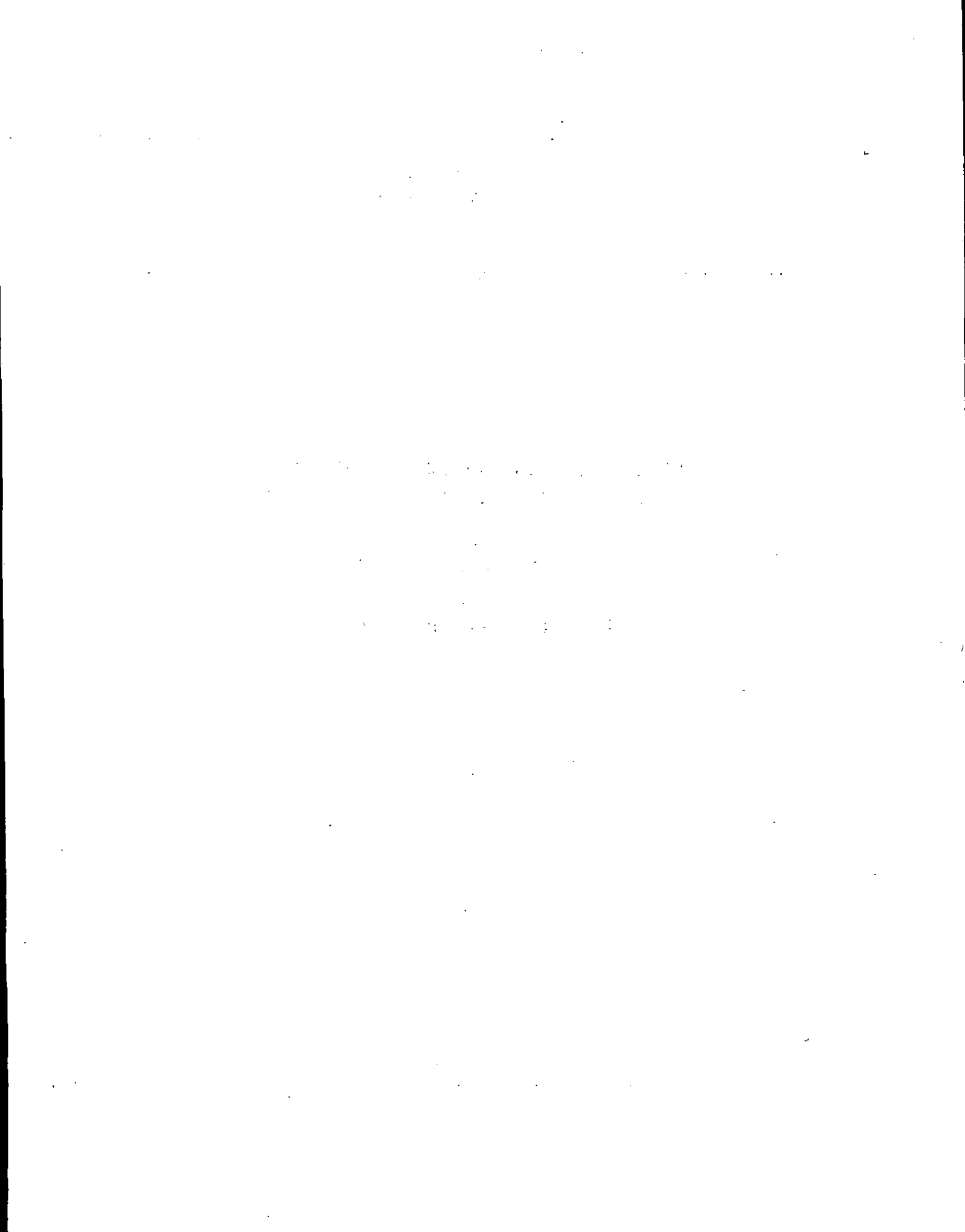
By

R. D. Mac Nish and R. A. Barker

of the
United States Geological Survey

Prepared cooperatively by the
UNITED STATES GEOLOGICAL SURVEY

1976



CONTENTS

	Page
Abstract-----	1
Introduction-----	2
Purpose and scope-----	2
Location-----	4
Previous work and acknowledgments-----	5
Primary aquifer system-----	5
Hydraulic characteristics-----	5
Flow system-----	6
Digital model-----	19
Characteristics-----	19
Relationship of the digital model to the primary aquifer system-----	25
Water levels (steady-stage conditions)-----	25
Transmissivity-----	26
Upper and lower confining layers-----	26
Storage coefficient-----	30
Pumpage-----	32
Aquifer boundaries-----	34
Steady-state model-----	34
Transient model-----	37
Observed and calculated response to stress-----	39
Projection based on 1972 pumpage-----	44
Limitations and areas for future investigations-----	49
References cited-----	50

ILLUSTRATIONS

	Page
PLATE 1. Map of subarea 4 showing water-level contours in January 1972 (in pocket)	(in pocket)
FIGURES 1-3. Maps showing:	
1. Walla Walla River basin and areal coverage of the digital model of the primary basalt aquifer system--	3
2. Water levels in the primary basalt aquifer system in 1900-----	8
3. Hydrologic subareas and the grid used in the digital simulation model-----	9
4. Schematic diagram showing head relationships and the resultant patterns of flow in the study area-----	11
5. Example graph of an algebraic approximation of a continuous function-----	20
6. Diagram of nodal array used in the digital model-----	21
7. Map showing transmissivity distribution used in the model-----	27
8. Map showing storage coefficient distribution in the model-----	31
9. Graph showing monthly distribution of irrigation electric power demand-----	32
10. Graph showing annual pumpage from the primary aquifer system-	33
11. Map showing water-level contours and calculated water levels for steady-state model in 1900-----	36
12. Map showing head distribution generated by the model in 1972--	40
13-15. Hydrographs for the period 1962-72 of nodes centered in:	
13. T.7 N., R.36 E., sec.17-----	41
14. T.7 N., R.35 E., sec.35-----	42
15. T.5 N., R.35 E., sec.12-----	43
16. Map showing 1980 water levels generated by the model-----	45
17-19. Hydrographs for the period 1972-80 of nodes centered in:	
17. T.7 N., R.36 E., sec.17-----	46
18. T.7 N., R.35 E., sec.35-----	47
19. T.5 N., R.35 E., sec.12-----	48

TABLES

TABLE 1. Selected wells penetrating basalt aquifer zones-----	12
2. Time-step equivalents of real time-----	38
3. Study-area water budgets in 1900 and 1972-----	44

The following factors are provided for conversion of English values used in this report to metric values:

<u>Multiply</u>	<u>By</u>	<u>To obtain</u>
Acre-feet----- (acre-ft)	1233.6	cubic metres (m ³)
Acre-feet per year----- (acre-ft/yr)	3.911x10 ⁻⁵	cubic metres per second (m ³ /s)
Feet (ft)-----	0.3048	metres (m)
Feet per second (ft/s)-----	0.3048	metres per second (m/s)
Feet squared per second----- (ft ² /s)	0.0929	metres squared per second (m ² /s)
Miles-----	1.609	kilometres (km)

DIGITAL SIMULATION OF A BASALT AQUIFER SYSTEM,
WALLA WALLA RIVER BASIN, WASHINGTON AND OREGON

By R. D. Mac Nish and R. A. Barker

ABSTRACT

A digital (mathematical) model utilizing an alternating-direction implicit procedure simulates the hydraulic response to 72 years of pumping stress of a basalt aquifer system underlying the 1,758-square-mile Walla Walla River basin in Washington and Oregon. The modeled aquifer system is sandwiched between an underlying basalt-aquifer zone and an overlying aquifer zone composed of gravel and clay in the central lowland part of the basin and of basalt elsewhere.

A water budget of the aquifer system before pumping stress began in about 1900 was computed by steady-state simulation. For this simulation the aquifer received 132,000 acre-feet of water per year, with 114,000 acre-feet entering from the principal recharge area, the Blue Mountains, on the southeastern border of the basin. Annual discharge rates were 97,500 acre-feet laterally to the Snake and Columbia Rivers and 34,500 acre-feet to adjacent aquifers, which also eventually drain to the two rivers.

By 1945 pumping stress had reached about 5,000 acre-feet per year. A large increase in irrigation demand over the next 20 years increased the pumpage to 20,000 acre-feet per year and caused declines of as much as 135 feet from the 1900 water levels. Simulation of the effects of pumping indicated that by 1972 the water budget of the basalt aquifer system showed a net increase of flow from the recharge areas (6,500 acre-feet per year) and reduction in both lateral outflow (8,500 acre-feet per year) and discharge to adjacent aquifers (12,500 acre-feet per year).

As calibrated, the model appears to have simulated the response of the aquifer system to the historical record of stress in the central lowland part of the basin with reasonable accuracy, and it could be used to project the effects of present and moderate additional stresses in the near future in this area. A shortcoming of the model is that an empirical method is used to approximate vertical fluxes to and from the aquifer.

INTRODUCTION

Purpose and Scope

In the late 1960's, growing concern over ground-water-level declines in the Walla Walla River basin in Washington and Oregon prompted the Washington State Department of Ecology (then the Department of Water Resources) to propose a cooperative hydrologic study of the area with the U.S. Geological Survey. The twofold purpose of the study was to (1) determine the water budget for the entire river basin, including those parts of the basin in the State of Oregon and (2) develop a digital model to simulate the aquifer system underlying the basin, with predictive capability for use as a management tool.

When the study began in 1970 the plan was to construct a single model of the complex aquifer system, which includes two major aquifers. However, it soon became apparent that it would be quicker and more economical to develop separate models, one for each of the aquifer systems. This report, the second of three planned reports on the progress and results of this investigation, deals with the basalt aquifer, the more extensive of the two.

The first report, by Mac Nish, Myers, and Barker (1973), described in general terms the hydrology of the Walla Walla River basin and the historical trends in development of the basin's ground-water resources. In addition, the first report satisfied the objective of defining the water budget for the basin. This report describes a digital model developed to simulate the basalt-aquifer system in the study area. The third and final report describes the digital model of the overlying gravel aquifer.

Location

The Walla Walla River basin is in southeastern Washington and northeastern Oregon, as shown in figure 1. Of the total drainage area of 1,758 square miles, 1,275 square miles are in Washington.

The basalt-aquifer system modeled and described in this report is only a small part of the volcanic-rock sequence which underlies the physiographic province of the Columbia Plateau (Fenneman, 1931, p. 225). Because the aquifer system is continuous across physiographic divides, the area modeled was expanded to the Snake, Umatilla, and Columbia Rivers, which act as boundaries to ground-water flow in the area. Therefore, the extent of the modeled area shown in figure 1 is larger than the Walla Walla River basin, although it does exclude some of the higher parts of the basin.

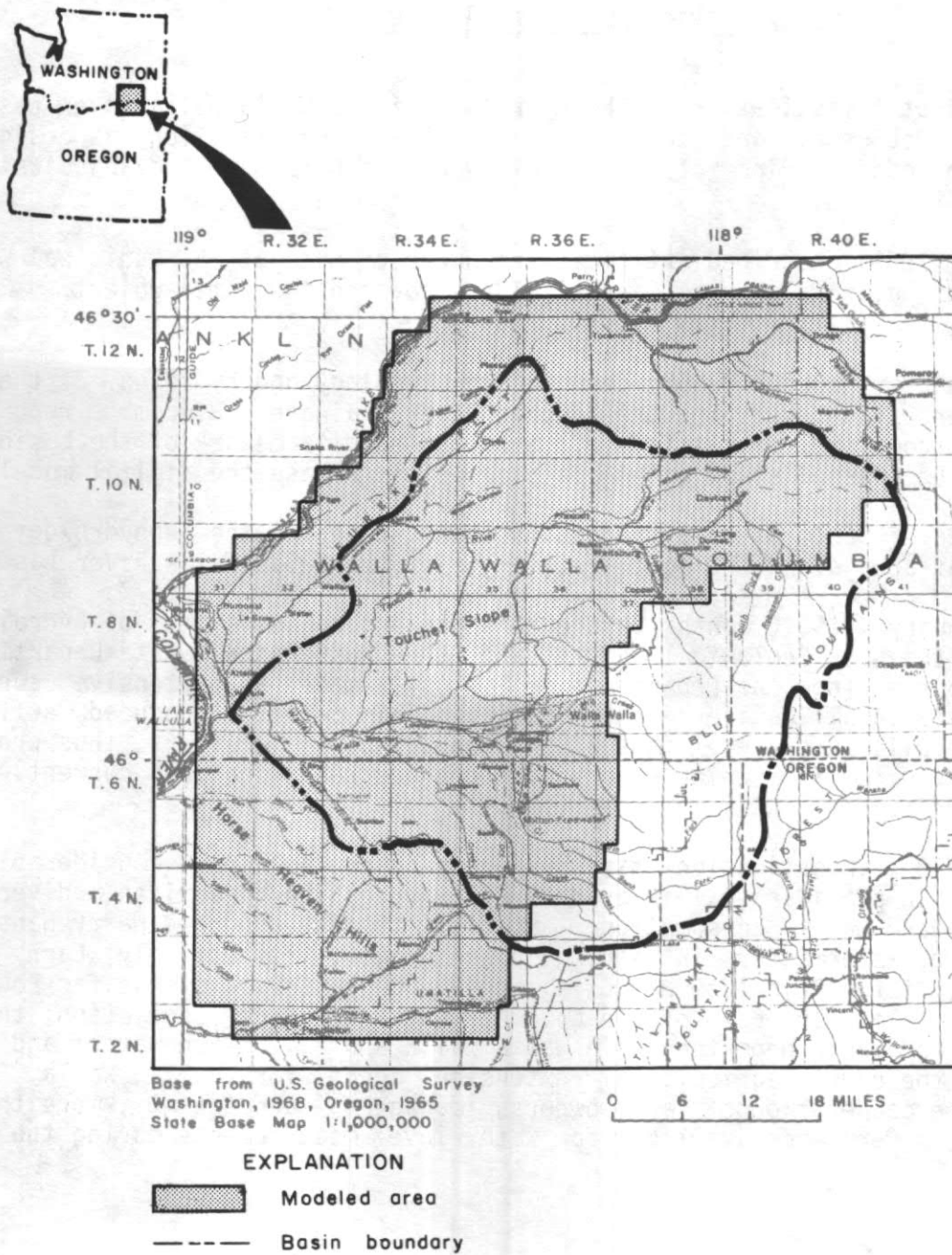


FIGURE 1.--Walla Walla River basin boundaries and areal coverage of the digital model of the primary basalt aquifer system.

Previous Work and Acknowledgments

The first investigation of the hydrology of the Walla Walla River basin was by Piper, Robinson, and Thomas (1933). Their investigation was designed to develop an understanding of the hydrology on which to base the adjudication of water rights.

Price (1961) described artificial-recharge efforts at a municipal well in the city of Walla Walla, and Garrett (1962) covered the same subject.

A report by Newcomb (1965) describes the geology and hydrology of the Walla Walla River basin, excluding the Touchet River drainage. Newcomb's report has the most complete discussion of the geologic framework of the basin, and provided the present study with data upon which to base the digital models.

Molenaar (1968) made a reconnaissance study of the geohydrology of the Eureka Flat area along the northwest margin of the Walla Walla River basin.

In January 1969, 6 months before this project began, a team of hydrologists from both the U.S. Geological Survey and the Washington State Department of Water Resources (now the Department of Ecology) made an extensive survey of water levels in all aquifers of the basin. This effort produced sufficient data to compile water-level maps of the two principal aquifers, thus providing a reference datum from which water-level changes resulting from current pumpage were determined.

During the investigation many residents of the area gave considerable time and effort in providing valuable data on irrigation practices, diversions, power use, and water consumption. Special thanks are due Harry Hansen and Robert Isit, watermasters in Washington and Oregon, respectively; Larry Ouzts, Jack Bean, Victor Reynolds, Ben Elia, and George Patterson of Pacific Power and Light Co.; Elmer Thompson of the Columbia Rural Electric Association; the city engineers and their departments in Walla Walla and Milton-Freewater; and Robert Williams, the county agricultural extension agent for Walla Walla County. Through the cooperation of farm owners, managers, and tenants, more than 160 basalt wells were made available for water-level measurements during the study.

PRIMARY AQUIFER SYSTEM

Hydraulic Characteristics

The modeled area shown in figure 1 is underlain by about 3,000 feet of layered basalt of the Columbia River Group. This basalt sequence is a thick accumulation of individual lava flows that taper and overlap laterally. Individual flows may reach a maximum of 150 feet in thickness.

Contact (interflow) zones between the successive flows, resulting from interruptions of flow during the outpouring of the basaltic lavas, comprise about 10 percent of a typical section in the basalt (Newcomb, 1965, p. 29). Because contact zones between individual lava flows are generally rubbly, containing angular, broken material, they provide conduits through which ground water may be readily transmitted.

In contrast to the horizontal permeable zones, many lava flows, especially the thinner flows, are traversed vertically by narrow cracks that developed as the lava contracted during cooling. Water transmission through these joints occurs very slowly in comparison to flow through the horizontal conduit zones in the basalt. Thus, the occurrence and movement of water in the basalt is greatly influenced by the physical nature of the flows and associated inter-zones.

The ability of a unit area of an aquifer to transmit water may be measured and described as its hydraulic conductivity. The hydraulic conductivity of horizontal permeable zones may be as large as 5 ft/s, while the vertical hydraulic conductivity may be as small as 0.00000005 ft/s. In other words, the rates of horizontal flow in the basalt may be as much as a billion times greater than for vertical flow through the basalt.

In places the sequence of basalt flows has been disrupted by movements of the earth's crust which occurred after the flows were laid down. Some of these disruptions are exemplified by the bending and warping of flows and interflow zones. In other places more intense disruptions have produced cracks that may traverse vertically through several flows and extend thousands of feet horizontally. When such folds "pinch off" porous interflow zones, or earth movement along the cracks offsets the interflow zones or plugs them with finely pulverized rock, these blockages can significantly reduce the rates of transmission of ground water.

Flow System

Gravity is the principal driving force for natural flow of water. Thus, the potential energy of a water particle is directly proportional to its elevation--the higher a particle's elevation, the greater its potential energy. However, the level at which water stands in a well represents the average potential energy of water in the part of the aquifer that the well penetrates. The areal distribution of these individual water levels constitutes a potentiometric surface. Although the pattern of flow in any small part of an aquifer system depends upon the physical and structural nature of the rock materials and directions of flow may vary greatly over small distances, water in an aquifer always moves from areas of high potential energy to those of low potential energy.

The basalt-aquifer system is a layered series of highly conductive aquifer zones alternating with dense basalt zones of very low hydraulic conductivity. Because most wells drilled into the basalt sequence underlying the study area are uncased and penetrate several permeable zones, they are open to more than one aquifer. The resulting static water levels represent an average or composite total head, which is influenced by all saturated zones open to the well bore. Alone, each aquifer zone would display a somewhat different potentiometric surface, and each would be bounded by the areal limits of the interflow zone it represented. This phenomenon is discussed more extensively by Luzier and Burt (1974).

Owing to the complex nature of this system, present data are inadequate to define a potentiometric surface for each aquifer zone in the basalt. In order to expedite the modeling effort, potentiometric surfaces for the basalt-aquifer system were developed using the following procedures:

1. Water levels from all available wells tapping the basalt aquifer were plotted on maps.
2. The maps were examined to compare the water levels in each well with those of nearby wells. Most basalt wells in the area where the land surface is below 1,300 feet above mean sea level tap a group of aquifer zones which, though individually discontinuous, are interconnected to the degree that they act as a single aquifer system. This group of basalt-aquifer zones is referred to in this report as the primary aquifer system.
3. Anomalous water-level data were examined to determine the cause of the anomaly. Most wells with anomalous water levels did not tap the same aquifer zones as the nearby wells. Composite heads also caused water levels in some wells to be displaced from the levels reflected in nearby wells. For some wells, it was possible to reconstruct the water level in the primary aquifer system when adequate information on water levels and yields during drilling were available. When such reconstruction was not possible, the anomalous water-level data were not included in the analysis.

The potentiometric surface shown in figure 2 is an expression of two-dimensional distribution of potential energy--the approximate water levels--in the primary aquifer system in 1900. Using historical water-level data the map in figure 2 was developed as an approximation of conditions in the primary aquifer system prior to the onset of pumping. Due to annual and seasonal changes in pumping rates, steady-state conditions have not existed since the first production well was drilled near the beginning of the century. As a result, the determination of the original steady-state water levels required some simplifying assumptions, the most important being that until the first wells were drilled in any particular area of the basin, the initial steady-state water levels were not significantly disturbed. Thus, the potentiometric map of the primary aquifer system is derived from static-water-level information at the time of drilling the very earliest wells in any particular area.

Ground-water-level data are sparse outside the central lowland (subarea 4 in fig. 3). Therefore, water-level contours shown outside the central lowland in figure 2 are more generalized than those within the central lowland. In the Touchet Slope-Eureka Flat area (subarea 8 of fig. 3) and upslope from the 1,200-foot water-level contour (subarea 5), the water-level contours of figure 2 are based on very few data. Water-level contours in subarea 7 (the Horse Heaven Hills area) are generally valid; however, locally they may be 20 feet or more in error.

The distribution of head potential in the aquifer system depends primarily on where water is added to or discharged from the aquifer. The Blue Mountains are the primary recharge area (where water is added to the flow system), whereas the Columbia and Snake River areas are the primary discharge areas of the aquifer system. Thus, the direction of ground-water flow in the primary aquifer system is generally northwestward from the high potentiometric surface along the southeastern margin of the area toward the areas of the low potentiometric surface in the vicinity of the Columbia and Snake Rivers (fig. 2).

The variations in head gradient within the basin are in part a result of the occurrence of secondary areas of recharge and discharge and in part due to the effects of the areal variations in the hydraulic characteristics of the aquifer itself. Areas of steep gradients indicate low values of hydraulic conductivity or a high net exchange of water to an aquifer zone above or below. In areas of low gradients, the hydraulic conductivity is likely to be high, or the net exchange of water to other aquifer zones is small.

The relationship of the primary aquifer system to overlying and underlying aquifer zones must be examined in order to determine the manner in which water enters and leaves the primary aquifer system. Present knowledge of the system is not adequate to quantify precisely the various hydraulic factors in the flow system, but enough evidence exists to demonstrate its nature in a qualitative fashion.

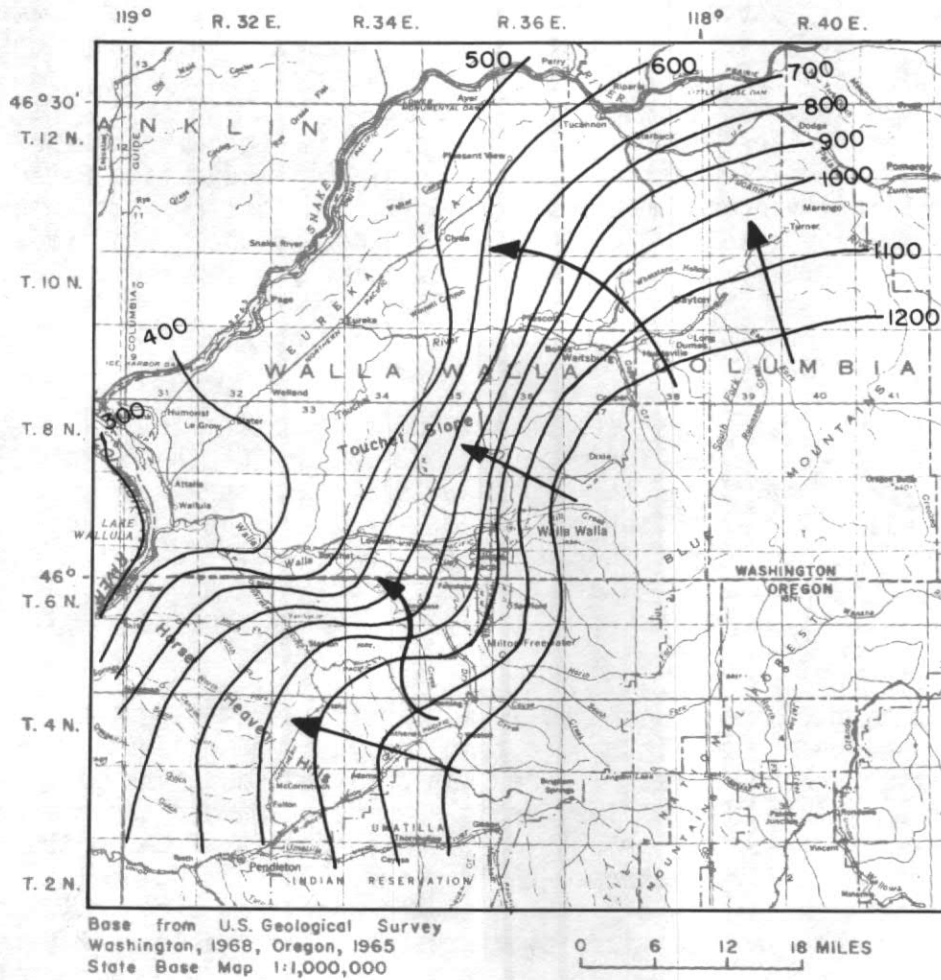


FIGURE 2.--Water-level contours of the primary basalt aquifer system in 1900, as reconstructed from the earliest available well data in the Walla Walla River basin. Arrows indicate general direction of ground-water movement.

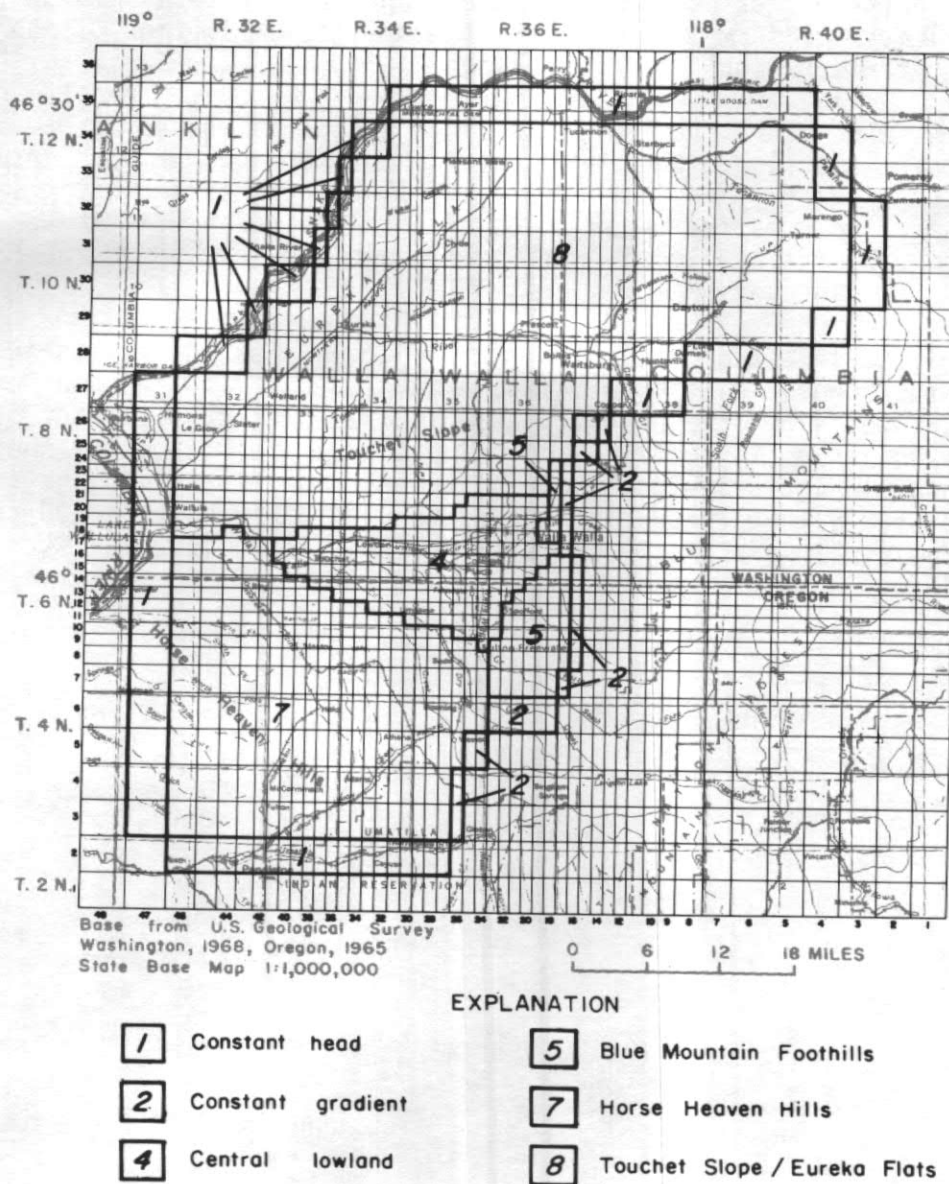


FIGURE 3.--Hydrologic subareas and boundaries and grid used in the digital model

Figure 4 shows, schematically, the distribution and head relationships between the primary aquifer system and the overlying and underlying aquifer zones. The relationships depicted in figure 4 are substantiated by data, except for the relationship between the lower aquifer zone and the primary aquifer system beneath the areas represented as sections A, B, C, and D. Few wells exist in these areas and none of them appears to penetrate any aquifers below the primary aquifer system. Thus, the areal distribution of the heads in the lower aquifer zone could not be defined.

Figure 4 shows that the primary aquifer system gains and loses water from both the upper and lower aquifer zones. The upper aquifer zone includes the gravel and underlying clay in the central lowland part of the basin (subarea 4 in fig. 3), and includes the upper zones of basalt elsewhere in the basin. The upper aquifer zone is largely a water-table aquifer, except in the Blue Mountains where artesian pressures are present.

Table 1 lists selected wells in the modeled area, noting their relative location in the schematic diagram (fig. 4) and identifying the aquifer zone or zones that the wells penetrate. For example, the first well listed taps the primary aquifer system in section G of figure 4. The table also gives the township-range and latitude-longitude locations, and information that the well is 1,000 feet deep, the altitude of the bottom of the hole is 300 feet above msl (mean sea level), and the water level was 910 feet above msl when measured in January 1970.

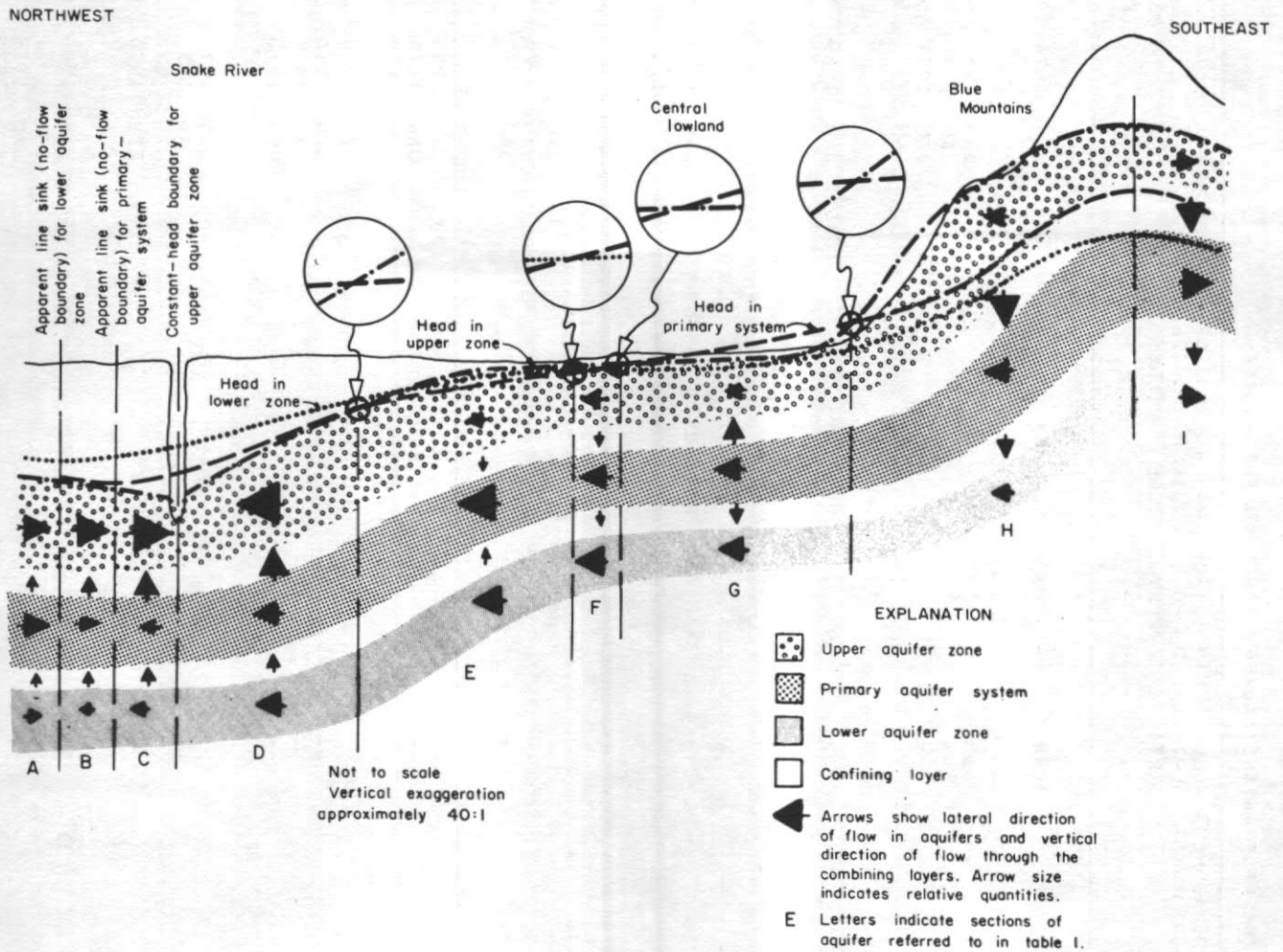


FIGURE 4.--Head relationships in major basalt aquifer zones and the resultant directions of ground-water flow in and between the aquifer zones in the modeled area.

TABLE 1.-- RECORDS OF SELECTED WELLS PENETRATING AQUIFER ZONES IN THE BASALT

TOWNSHIP/RANGE SECTION	LATITUDE	LONGITUDE (S)	NODE NORTH	ADDRESS WEST	WELL DEPTH (FT)	DEPTH CASED (FT)	BOTTOM HOLE ELEV. MSL (FT)	MAJOR AQUIFER ZONE	MINOR AQUIFER ZONES	YIELD (GPM)	MONTH	YEAR	W/L ELEV. MSL (FT)	SECTION (FIG.4)
05N/35E-26F01	45°53' 6"N	118°24'14"W(1)	7	25	1000	--	300	PRIMARY		--	JAN	1970	910	G
05N/35E-12001	45°55'12"N	118°22'46"W(1)	8	24	918	--	243	PRIMARY		--	JAN	1969	908	G
					--		--				JAN	1970	917	
					--		--				JAN	1971	913	
					--		--				JAN	1972	911	
05N/35E-12F02	45°55'40"N	118°23' 5"W(1)	9	24	902	99	160	PRIMARY		1000	JAN	1969	864	G
					--		--				JAN	1971	856	
					--		--				JAN	1972	836	
					--		--				FEB	1973	846	
05N/35E-01C02	45°56'40"N	118°22'55"W(1)	10	24	348	334	680	PRIMARY	UPPER	55	JAN	1970	852	H
					--		--				JAN	1971	865	
					--		--				JAN	1972	859	
05N/35E-06D01	45°56'49"N	118°29'26"W(1)	10	30	625	202	170	PRIMARY		736	JAN	1969	720	G
					--		--				JAN	1970	722	
					--		--				JAN	1971	719	
					--		--				JAN	1972	718	
06N/34E-36N01	45°57' 3"N	118°30'41"W(1)	11	31	300	255	448	PRIMARY		1200	JAN	1969	719	G
					--		--				JAN	1970	718	
06N/35E-31F01	45°57'20"N	118°29'15"W(1)	11	29	970	748	-222	PRIMARY	LOWER	515	JAN	1969	688	G
					--		--				JAN	1970	686	
					--		--				JAN	1971	687	
					--		--				FEB	1973	686	
06N/36E-32E01	45°57'30"N	118°20'58"W(1)	11	23	920	--	35	LOWER	PRIMARY	2000	JAN	1970	736	H
					--		--				JAN	1971	726	
					--		--				JAN	1972	723	
					--		--				FEB	1973	720	
06N/34E-35C01	45°57'30"N	118°31'48"W(1)	11	31	476	90	224	PRIMARY	UPPER	950	JAN	1969	681	F
					--		--				JAN	1971	676	
					--		--				JAN	1972	674	
					--		--				FEB	1973	676	

TABLE 1 (CONT'D).-- RECORDS OF SELECTED WELLS IN THE BASALT

TOWNSHIP/RANGE SECTION	LATITUDE	LONGITUDE (S)	NODE NORTH	ADDRESS WEST	WELL DEPTH (FT)	DEPTH CASED (FT)	BOTTOM HOLE ELEV. MSL (FT)	MAJOR AQUIFER ZONE	MINOR AQUIFER ZONES	YIELD (GPM)	MONTH	YEAR	W/L ELEV. MSL (FT)	SECTION (FIG.4)
06N/34E-35D01	45°57'36"N	118°32'12"W(1)	11	32	697	60	-39	PRIMARY	UPPER	2100	JAN	1969	645	F
					--	--	--					JAN 1970	634	
					--	--	--					JAN 1971	644	
					--	--	--					FEB 1973	646	
06N/35E-28C02	45°58'29"N	118°26'53"W(1)	12	27	1050	--	-268	PRIMARY	LOWER	200	JAN	1969	730	G
					--	--	--					JAN 1971	732	
					--	--	--					JAN 1972	732	
06N/35E-23D01	45°59'16"N	118°24'37"W(1)	13	26	1007	687	-184	PRIMARY	UPR&LOWR	150	JAN	1969	760	G
					--	--	--					JAN 1970	757	
					--	--	--					JAN 1972	751	
					--	--	--					FEB 1973	747	
06N/35E-13R01	45°59'29"N	118°22'15"W(1)	13	24	1030	--	-210	LOWER	PRIMARY	536	JAN	1969	748	H
					--	--	--					JAN 1972	734	
					--	--	--					FEB 1973	729	
06N/33E-15R01	45°59'49"N	118°39'52"W(1)	14	38	650	--	-100	PRIMARY	--	--	JAN	1970	459	F
06N/36E-14E01	45°59'58"N	118°16'58"W(1)	14	19	614	250	551	PRIMARY		18	JAN	1970	950	H
					--	--	--					JAN 1971	953	
					--	--	--					JAN 1972	951	
					--	--	--					FEB 1973	947	
06N/35E-12N01	46° 0'20"N	118°22'57"W(1)	14	24	590	--	178	LOWER	PRIMARY	--	JAN	1964	743	G
					--	--	--					JAN 1970	743	
					--	--	--					JAN 1971	736	
					--	--	--					FEB 1973	730	
06N/36E-10J03	46° 0'35"N	118°17'15"W(1)	15	20	640	516	478	PRIMARY		900	JAN	1969	963	H
06N/36E-09L01	46° 0'39"N	118°18'51"W(1)	15	21	1155	939	-149	LOWER	PRIMARY	1240	JAN	1970	835	H
					--	--	--					JAN 1971	826	
					--	--	--					JAN 1972	824	
					--	--	--					FEB 1973	821	

PRIMARY AQUIFER SYSTEM

TABLE 1 (CONT'D).-- RECORDS OF SELECTED WELLS IN THE BASALT

TOWNSHIP/RANGE SECTION	LATITUDE	LONGITUDE (S)	NODE ADDRESS NORTH WEST	WELL DEPTH (FT)	DEPTH CASED (FT)	BOTTOM HOLE ELEV. MSL (FT)	MAJOR AQUIFER ZONE	MINOR AQUIFER ZONES	YIELD (GPM)	MONTH	YEAR	W/L ELEV. MSL (FT)	SECTION (FIG.4)
06N/33E-07J02	46° 0'49"N	118°43'20"W(1)	15 41	150	138	334	UPPER		350	JAN	1969	454	E
				--		--				JAN	1970	460	
				--		--				JAN	1971	464	
				--		--				JAN	1972	458	
06N/33E-07J01	46° 0'49"N	118°43'24"W(1)	15 41	150	12	342	UPPER		350	JAN	1970	470	E
				--		--				JAN	1971	473	
06N/36E-12A01	46° 1' 1"N	118°14'46"W(1)	15 18	795	--	550	UPPER		--	JAN	1970	1162	H
06N/34E-07R02	46° 1' 5"N	118°36'14"W(2)	15 35	1340	950	-845	LOWER	PRIMARY	1080	JAN	1969	432	F
				--		--				JAN	1970	424	
				--		--				JAN	1971	424	
				--		--				JAN	1972	422	
06N/32E-01R01	46° 1'28"N	118°44'48"W(1)	16 41	1000	--	-550	LOWER	PRIMARY	--	JAN	1969	429	E
06N/37E-05F01	46° 1'40"N	118°12'34"W(1)	16 16	612	125	943	UPPER		2390	JAN	1969	1704	H
06N/33E-05M02	46° 1'41"N	118°43' 8"W(1)	16 40	146	120	273	PRIMARY	UPPER	--	JAN	1971	408	E
				--		--				FEB	1973	408	
06N/35E-01C01	46° 2' 0"N	118°22'39"W(1)	16 24	535	--	265	PRIMARY		500	JAN	1970	760	G
				--		--				JAN	1971	768	
				--		--				JAN	1972	770	
				--		--				FEB	1973	776	
06N/35E-01C03	46° 2' 4"N	118°22'49"W(1)	16 24	549	400	225	PRIMARY		500	JAN	1969	759	G
07N/36E-34N01	46° 2'11"N	118°18' 8"W(1)	16 20	505	409	485	PRIMARY	UPPER	340	JAN	1969	891	G
				--		--				JAN	1971	891	
				--		--				JAN	1972	887	
				--		--				FEB	1973	879	
07N/33E-31R02	46° 2'21"N	118°43'23"W(1)	17 41	320	--	176	PRIMARY		--	JAN	1969	400	E
				--		--				JAN	1970	401	
				--		--				JAN	1971	401	
				--		--				JAN	1972	400	

TABLE 1 (CONT'D).-- RECORDS OF SELECTED WELLS IN THE BASALT

TOWNSHIP/RANGE SECTION	LATITUDE	LONGITUDE (S)	NODE ADDRESS NORTH WEST	WELL DEPTH (FT)	DEPTH CASED (FT)	BOTTOM HOLE ELEV. MSL (FT)	MAJOR AQUIFER ZONE	MINOR AQUIFER ZONES	YIELD (GPM)	MONTH	YEAR	W/L ELEV. MSL (FT)	SECTION (FIG.4)
07N/35E-33L02	46° 2'22"N	118°26'23"W(1)	17 27	650	550	25	LOWER	PRIMARY	--	JAN	1969	624	G
07N/36E-31J01	46° 2'29"N	118°21' 2"W(1)	17 23	1715	538	-833	LOWER	PRIMARY	--	JAN	1964	774	G
				--		--				JAN	1971	769	
				--		--				JAN	1972	767	
				--		--				FEB	1973	762	
07N/36E-33D02	46° 2'52"N	118°19'22"W(1)	17 21	1412	1285	-492	LOWER	PRIMARY	2600	JAN	1972	823	G
07N/35E-33D01	46° 2'53"N	118°26'41"W(1)	17 27	760	617	-95	LOWER	PRIMARY	310	DEC	1945	655	G
				--		--				JAN	1969	604	
07N/35E-35A01	46° 2'54"N	118°23'23"W(1)	17 25	1022	610	-237	PRIMARY	LOWER	185	APR	1960	791	G
				--		--				JAN	1970	745	
				--		--				JAN	1971	732	
				--		--				JAN	1972	728	
07N/35E-31B01	46° 2'56"N	118°28'47"W(1)	17 29	1104	665	-459	PRIMARY	LOWER	840	JAN	1969	603	G
				--		--				JAN	1971	598	
				--		--				JAN	1972	600	
				--		--				FEB	1973	596	
07N/34E-26R01	46° 3' 2"N	118°31' 2"W(1)	18 31	460	145	115	PRIMARY	UPPER	455	JAN	1969	537	G
				--		--				JAN	1970	538	
				--		--				JAN	1971	538	
07N/34E-25N01	46° 3' 3"N	118°30'35"W(1)	18 30	1102	180	-522	LOWER	PRIMARY	442	JAN	1969	534	G
				--		--				JAN	1970	534	
				--		--				JAN	1971	535	
				--		--				JAN	1972	532	
07N/36E-28R01	46° 3'11"N	118°18'20"W(1)	18 21	1090	300	-68	LOWER	PRIMARY	1725	JAN	1969	877	H
07N/33E-26L01	46° 3'19"N	118°39' 1"W(1)	18 37	863	538	-285	LOWER	PRIMARY	400	JAN	1969	471	E
				--		--				JAN	1970	469	
				--		--				JAN	1971	465	
				--		--				JAN	1972	463	

PRIMARY AQUIFER SYSTEM

TABLE 1 (CONT'D).-- RECORDS OF SELECTED WELLS IN THE BASALT

TOWNSHIP/RANGE SECTION	LATITUDE	LONGITUDE (S)	NODE ADDRESS NORTH WEST	WELL DEPTH (FT)	DEPTH CASED (FT)	BOTTOM HOLE ELEV. MSL (FT)	MAJOR AQUIFER ZONE	MINOR AQUIFER ZONES	YIELD (GPM)	MONTH	YEAR	W/L ELEV. MSL (FT)	SECTION (FIG.4)
07N/36E-25E01	46° 3'27"N	118°15'24"W(1)	18 18	1100	157	234	PRIMARY	UPPER	690	JAN	1971	1053	H
				--	--	--				JAN	1972	1060	
				--	--	--				FEB	1973	1056	
07N/36E-27G01	46° 3'35"N	118°17'23"W(1)	18 20	450	357	630	UPPER	PRIMARY	224	JAN	1969	1044	H
				--	--	--				JAN	1970	1039	
				--	--	--				JAN	1971	1044	
				--	--	--				FEB	1973	1040	
07N/34E-28E01	46° 3'35"N	118°34'16"W(2)	18 33	834	44	-292	LOWER	PRIMARY	420	JAN	1970	454	F
				--	--	--				JAN	1971	454	
				--	--	--				JAN	1972	454	
				--	--	--				FEB	1973	454	
07N/35E-26R02	46° 3'37"N	118°23'49"W(1)	18 25	650	--	128	PRIMARY	LOWER	--	JAN	1969	735	G
07N/35E-25A01	46° 3'39"N	118°22'18"W(1)	18 24	652	547	200	PRIMARY	LOWER	170	JAN	1969	785	G
				--	--	--				JAN	1972	729	
				--	--	--				FEB	1973	724	
07N/34E-30A01	46° 3'40"N	118°36' 0"W(1)	18 35	601	40	-113	PRIMARY	LOWER	560	JAN	1969	423	F
				--	--	--				JAN	1970	421	
				--	--	--				JAN	1971	417	
				--	--	--				JAN	1972	414	
07N/34E-29C01	46° 3'41"N	118°35' 7"W(1)	18 34	1201	610	-696	UPPER	LOWER	1056	JAN	1970	426	F
				--	--	--				JAN	1971	424	
				--	--	--				JAN	1972	419	
				--	--	--				FEB	1973	421	
07N/33E-24Q01	46° 3'52"N	118°37'17"W(1)	19 36	1000	--	-482	PRIMARY	UPR&LOWR	--	JAN	1969	439	F
				--	--	--				JAN	1970	434	
				--	--	--				JAN	1971	433	
				--	--	--				JAN	1972	427	
07N/36E-19R01	46° 3'57"N	118°20'48"W(1)	18 23	1590	560	-665	LOWER		1134	JAN	1969	740	G
				--	--	--				JAN	1970	718	
				--	--	--				JAN	1971	711	
				--	--	--				FEB	1973	702	

TABLE 1 (CONT'D).-- RECORDS OF SELECTED WELLS IN THE BASALT

TOWNSHIP/RANGE SECTION	LATITUDE	LONGITUDE (S)	NODE ADDRESS NORTH WEST	WELL DEPTH (FT)	DEPTH CASED (FT)	BOTTOM HOLE ELEV. MSL (FT)	MAJOR AQUIFER ZONE	MINOR AQUIFER ZONES	YIELD (GPM)	MONTH	YEAR	W/L ELEV. MSL (FT)	SECTION (FIG.4)
07N/34E-21M01	46° 4' 8"N	118°34'26"W(1)	19 33	240	40	295	LOWER	PRIMARY	--	JAN	1969	437	F
				--		--				JAN	1971	431	
				--		--				JAN	1972	427	
07N/34E-22M01	46° 4'13"N	118°33' 8"W(1)	19 32	242	--	308	PRIMARY	UPPER	5	JAN	1971	520	F
				--		--				JAN	1972	519	
07N/36E-20H01	46° 4'21"N	118°19'44"W(1)	19 22	1202	--	-217	PRIMARY	LOWER	708	JAN	1969	868	G
				--		--				JAN	1972	859	
07N/36E-17L01	46° 4'57"N	118°20' 9"W(1)	20 22	2728	2155	***	PRIMARY	LOWER	140	JAN	1969	868	G
				--		--				JAN	1971	874	
07N/35E-14J01	46° 4'59"N	118°23'17"W(1)	20 24	1227	532	-352	LOWER	PRIMARY	1000	JAN	1969	737	G
				--		--				JAN	1971	725	
				--		--				JAN	1972	772	
07N/36E-13F02	46° 5'16"N	118°15'15"W(1)	20 18	808	140	442	PRIMARY	UPPER	822	JAN	1969	1089	H
07N/35E-07Q01	46° 5'36"N	118°28'38"W(1)	20 29	285	--	361	PRIMARY		--	JAN	1970	582	G
				--		--				JAN	1971	580	
				--		--				JAN	1972	580	
				--		--				FEB	1973	574	
07N/35E-08A01	46° 6'20"N	118°27'17"W(1)	21 28	780	--	-101	LOWER	PRIMARY	--	JAN	1969	502	G
				--		--				JAN	1970	499	
07N/33E-10A01	46° 6'28"N	118°39'39"W(1)	22 38	159	30	346	UPPER	PRIMARY	--	JAN	1969	410	E
07N/36E-02J01	46° 6'51"N	118°15'46"W(1)	22 18	810	164	425	UPPER	PRIMARY	1160	JAN	1969	1126	H
				--		--				JAN	1971	1122	
				--		--				JAN	1972	1125	
08N/37E-31P01	46° 7'22"N	118°14' 4"W(1)	22 17	99	25	1121	UPPER	PRIMARY	40	JAN	1969	1194	H
				--		--				FEB	1970	1198	
				--		--				JAN	1971	1184	
				--		--				JAN	1972	1189	

PRIMARY AQUIFER SYSTEM

TABLE 1 (CONT'D).-- RECORDS OF SELECTED WELLS IN THE BASALT

TOWNSHIP/RANGE SECTION	LATITUDE	LONGITUDE (S)	NODE NORTH	ADDRESS WEST	WELL DEPTH (FT)	DEPTH CASED (FT)	BOTTOM HOLE ELEV. MSL (FT)	MAJOR AQUIFER ZONE	MINOR AQUIFER ZONES	YIELD (GPM)	MONTH	YEAR	W/L ELEV. MSL (FT)	SECTION (FIG.4)
08N/35E-34001	46° 7'28"N	118°24'52"W(1)	23	26	1026	--	-276	LOWER	PRIMARY	1200	JAN	1969	718	G
08N/36E-35M02	46° 7'34"N	118°16'44"W(1)	23	19	540	222	580	UPPER	PRIMARY	284	JAN	1971	1031	H
09N/32E-29A01	46°14'23"N	118°49'37"W(1)	27	42	--	--	--	UPPER		--	FEB	1970	442	D
09N/32E-20D01	46°15' 8"N	118°50'31"W(1)	27	42	920	--	-417	UPPER	PRIMARY	--	AUG	1972	389	D
12N/38E-21L01	46°30'20"N	118° 4'10"W(1)	33	8	--	--	--	PRIMARY		--	AUG	1972	840	D
12N/38E-19C01	46°30'42"N	118° 6'31"W(1)	33	9	70	--	610	PRIMARY		--	AUG	1972	784	D
12N/38E-19C02	46°30'43"N	118° 6'38"W(1)	33	9	68	--	612	PRIMARY		--	AUG	1972	784	D
12N/34E-14R01	46°30'58"N	118°30'46"W(1)	34	27	1187	--	278	UPPER		--	AUG	1972	465	D
12N/35E-06K01	46°33' 0"N	118°28'43"W(1)	39	25	937	--	303	UPPER		--	JAN	1961	403	E
12N/34E-03H01	46°33'24"N	118°32'14"W(1)	34	28	202	165	341	UPPER		40	JAN	1971	438	D
13N/38E-27K01	46°34'50"N	118° 1'55"W(1)	35	7	381	330	262	PRIMARY		300	DEC	1963	626	D
13N/38E-27L02	46°34'50"N	118° 2'15"W(1)	35	7	381	320	194	PRIMARY		--	JUL	1972	637	D
13N/38E-27L01	46°34'51"N	118° 2' 4"W(1)	35	7	130	55	450	UPPER		350	AUG	1952	539	D
13N/38E-27H01	46°35' 5"N	118° 1'21"W(1)	35	7	204	80	406	UPPER		700	MAY	1953	551	D
13N/36E-19F01	46°35'55"N	118°20'41"W(1)	35	19	--	--	--	UPPER		--	AUG	1972	454	D
13N/40E-09C01	46°37'57"N	117°48'13"W(1)	36	3	175	134	515	UPPER		80	AUG	1969	578	D

DIGITAL MODEL

Characteristics

The digital model developed for the primary basalt aquifer in the study area shares many characteristics with other models developed for other aquifers. A rigorous mathematical description of the fundamental method, which uses the alternating-direction implicit procedure, was given by Pinder and Bredehoeft (1968).

The flow of ground water is often described by a partial differential equation of the form:

$$T \left(\frac{\partial^2 h}{\partial x^2} + \frac{\partial^2 h}{\partial y^2} \right) = S \frac{\partial h}{\partial t} + W(x,y,t) \quad (1)$$

where

- S = storage coefficient of the aquifer,
- h = head or water level in the aquifer,
- t = time,
- T = transmissivity of the aquifer,
- x and y = horizontal distances in mutually perpendicular directions, and
- W = rate of water movement to or from the aquifer vertically (flux).

This equation may be expressed literally as:

Rate of net lateral flow to and from some segment of the aquifer system	=	Rate of change of the volume of water stored in that segment	+	Rates at which water is being added to or removed from that aquifer segment ver- tically (e.g. as from wells).
--	---	---	---	---

An analytic solution of the equation would give the head "h" anywhere in the aquifer at any time. Unfortunately, present mathematical techniques are not adequate to find the analytic solution to this equation for many practical problems.

An alternative method used by this model substitutes a numerical approximation for the partial differential equation. The solution of this numerical approximation is not continuous in time and space as is the analytic solution. However, because high-speed digital computers can calculate the numerical substitutes so rapidly, it is possible to solve this approximation for small segments of aquifers over short time periods. Thus, the smaller the size of the aquifer segment, and the shorter the time period, the more closely the numerical substitute approximates the analytical solution. An example of a comparison of the two methods for a case where the solution can be found by both methods is shown in figure 5.

In order to construct a digital model it is necessary to subdivide the system being studied into discrete segments or elements, usually called cells or blocks, each having a node at its center. If the cells chosen are suitably small, the values of the hydraulic parameters describing the aquifer--transmissivity, storage coefficient, and water level--will not vary significantly within any single cell. A diagram of a part of the cell array is shown in figure 6 for a small part of the Walla Walla River basin. As shown in the example, water levels for the year 1900 are shown, one within each cell. Values for all hydraulic parameters used in the model are either measured, calculated, or estimated for each node lying within the modeled area.

The numbers along the margins of the grid of cells in the top diagram are the addresses of the nodes. For instance, the example cell shown in figure 6 has the address (16,22). This addressing system permits simplification of the computer programs because the same equation is solved at each node.

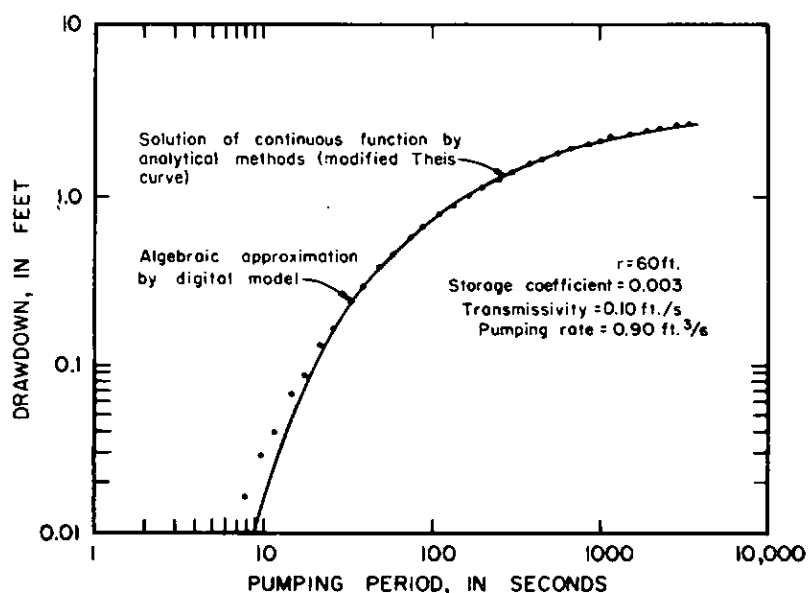
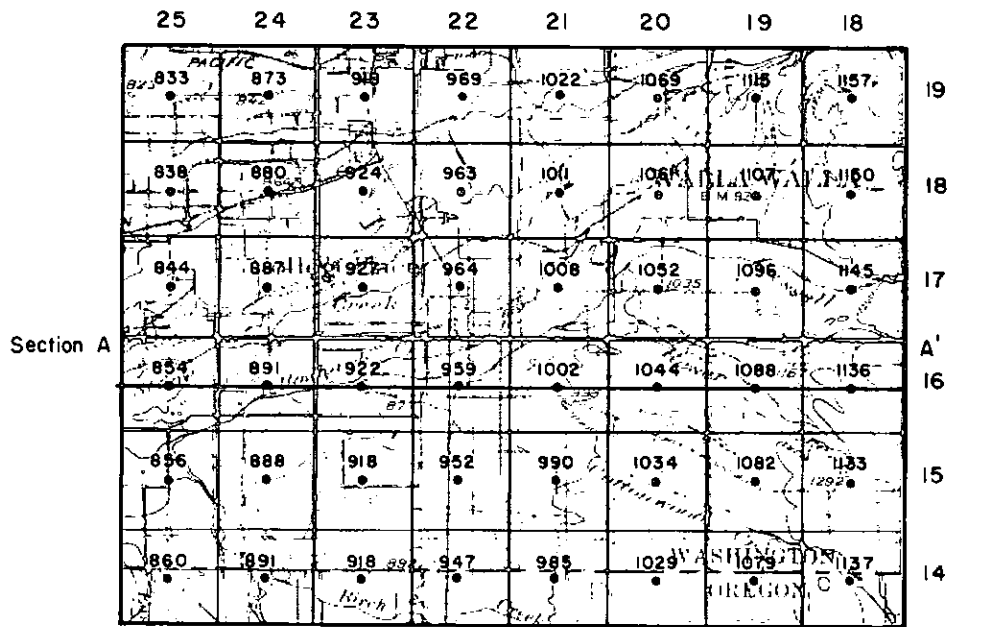
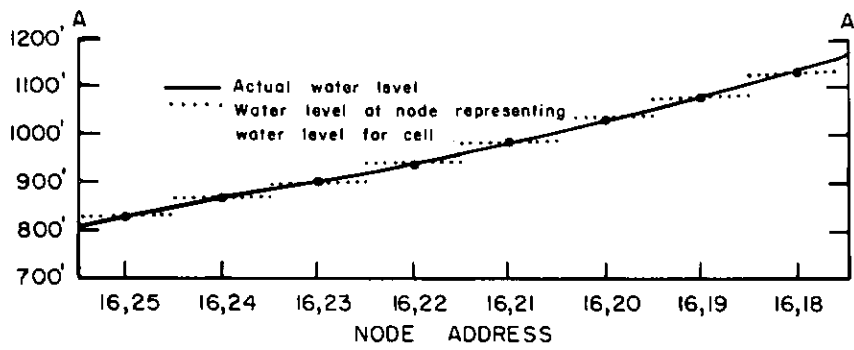
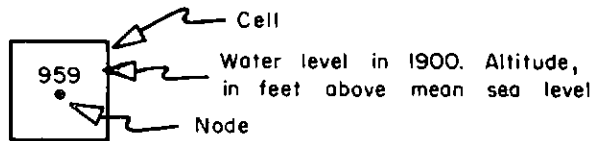


FIGURE 5.--Comparison of solutions of time-drawdown curve by analytical and algebraic approximation methods. Modified from Pinder and Bredehoeft (1968).



0 1 2 MILES
 CONTOUR INTERVAL 50 FEET
 DATUM IS MEAN SEA LEVEL

EXPLANATION



Datum is mean sea level
 Vertical exaggeration x 26.4

FIGURE 6.--Nodal array used in digital model of the primary basalt aquifer system.

Pinder and Bredehoeft (1968) provided the general equation for the numerical approximation of the partial differential equation (equation 1) as:

$$\begin{aligned}
 & \left(\frac{2T_{(i,j)} T_{(i+1,j)}}{T_{(i,j)} y_{(i+1)} + T_{(i+1,j)} y_{(i)}} \right) \left(\frac{h_{(i+1,j,t^*)} - h_{(i,j,t^*)}}{y_{(i)}} \right) \\
 + & \left(\frac{2T_{(i,j)} T_{(i-1,j)}}{T_{(i,j)} y_{(i-1)} + T_{(i-1,j)} y_{(i)}} \right) \left(\frac{h_{(i-1,j,t^*)} - h_{(i,j,t^*)}}{y_{(i)}} \right) \\
 + & \left(\frac{2T_{(i,j)} T_{(i,j+1)}}{T_{(i,j)} x_{(j+1)} + T_{(i,j+1)} x_{(j)}} \right) \left(\frac{h_{(i,j+1,t^*)} - h_{(i,j,t^*)}}{x_{(j)}} \right) \\
 + & \left(\frac{2T_{(i,j)} T_{(i,j-1)}}{T_{(i,j)} x_{(j-1)} + T_{(i,j-1)} x_{(j)}} \right) \left(\frac{h_{(i,j-1,t^*)} - h_{(i,j,t^*)}}{x_{(j)}} \right) \\
 & \text{----- lateral flow expression -----} \\
 = & S_{(i,j)} \left(\frac{h_{(i,j,t)} - h_{(i,j,t-1)}}{t - (t-1)} \right) \quad W_{(i,j,t-1)} \quad (2) \\
 & \text{----- storage term -----} \quad \text{-----vertical flow term-----}
 \end{aligned}$$

where the "(i,j)" subscripts are the addresses of the particular nodes at which the equations are solved.

The elements of the equation are:

- h = potentiometric head at a node,
- T = transmissivity,
- x and y = length and breadth of the node, and
- S = storage coefficient.

In the storage and vertical-flow terms, the "t-1" and "t" refer to the beginning and end, respectively, of the time period for which the equation is being solved. In the lateral-flow expression, t* represents a point in time between t and t-1.

The method of solution is to solve repetitively the equations at each node lying within the boundaries of the model for a particular time interval. In this model the direction of solution alternates between northerly and westerly on successive passes. After each pair of alternate-direction passes are computed, the differences between the two are compared. The sets of passes are repeated until these differences become so small as to be considered insignificant.

A more rigorous discussion of the mechanics of the solution was presented by Bredehoeft and Pinder (1970).

The vertical-flow term ($W_{(i,j,t-1)}$) in equation 2 includes all components of vertical flow into and out of a node. These components include the discharge of water through wells tapping the aquifer, and leakage to and from other aquifers above and below the primary basalt aquifer. Approximation of this term requires that, for the period of time over which the equations are being solved, the values comprised in the "W" term remain fixed. Because some components, such as pumpage, may vary greatly over a short period of time, as harvests and weather affect irrigation demand, the duration of the time intervals for which the equations are solved must be kept small. This characteristic of the model requires a high frequency of solution during any period when water levels are changing rapidly, as at the beginning, and after the end of the irrigation season.

Components of the "W" term in equation 2 are:

$$W_{(i,j)} = P_{(i,j)} + \frac{K}{M_{u(i,j)}} \left(h_{(i,j,t_0)} - h_{u(i,j,t_0)} \right) + \frac{K}{M_{l(i,j)}} \left(h_{(i,j,t)} - h_{l(i,j,t-1)} \right) \quad (3)$$

where

P = rate of pumpage at a particular node over the time interval of the solution,

K = hydraulic conductivity of the upper and lower confining layer,

M_u = thickness of the upper confining layer,

M_l = thickness of the lower confining layer,

t_0 = initial time,

t = current time,

$t-1$ = time at the previous time step,

h = head in the primary aquifer system,

h_u = head in the upper aquifer zone, and

h_l = head in the lower aquifer zone.

Input data to the model thus include:

1. Head distributions in the upper aquifer zone, primary aquifer system, and lower aquifer zone.
2. Transmissivity of the primary aquifer system.
3. Thicknesses and hydraulic conductivities of the upper and lower confining layers.
4. Storage coefficients of the primary aquifer system.
5. Pumping rates of wells in the primary aquifer system.
6. Boundary conditions at the model borders.

In the following section the development, distribution and accuracy of these input data are discussed.

Relationship of the Digital Model to the Primary Aquifer System

In the development of a mathematical model of a hydrologic system, the types of data needed and the limits of data availability often require compromises to facilitate model construction. This section of the report explains methods used to interpret the data and development of input data to the digital model and points out some of the important compromises involved in this process.

Water Levels (Steady-State Conditions)

After the water-level contour map for the primary aquifer system was developed for the year 1900 as described previously (p. 6), the value which approximated the average water level in each node of the model was placed in the model input data set. In the process, one of the more obvious compromises involved in digital simulation is encountered. This compromise is the approximation of a continuous function (in this case a water-level surface) by a series of point values. Referring back to figure 6, section A-A' shows both the actual water level in the basalt as a continuous curve and the values entered for each node along that section to approximate that curve. Obviously, a well could be located within a cell but have a water level somewhat different than the final value simulated for that cell. This must be kept in mind when comparing simulated water levels to water levels in wells.

Water-level data for the upper aquifer zone were available for most areas of the basin. In the central lowland (subarea 4 in fig. 3), the water levels in the gravel aquifer were used, whereas in all other subareas water levels in the basalt aquifers overlying the primary aquifer system were used.

Water-level data for the lower aquifer zone were not available for most of the study area. In the eastern part of the central lowland enough wells penetrated the lower aquifer zone so that a potentiometric surface for this zone could be approximated. Elsewhere in the model the heads were arbitrarily chosen as equal to the heads in the primary aquifer zone. The ramifications of this assumption are discussed in greater detail later (p. 29).

Transmissivity

Values of transmissivity used in the model were estimated for each cell. One aquifer test reported by Price (1960, p.29), indicated a transmissivity of $0.62 \text{ ft}^2/\text{s}$, and analysis of several unpublished aquifer tests on municipal wells in Walla Walla showed an average transmissivity value of $0.44 \text{ ft}^2/\text{s}$. It should be noted that these tests were made on the more highly productive wells in the basin. The values may be used as general upper limits of transmissivity in the model, as they are derived from wells open to all aquifer zones penetrated and reflect the transmissivity of the full thickness of the modeled zone and also parts of aquifer zones above and below the primary aquifer zone. Over the 1-square-mile area occupied by a cell, water in moving downgradient probably passes through zones of much lower transmissivity so that the transmissivity affecting the hydraulic gradient across an entire cell must reflect the transmissivity of the least transmissive zones through which the water must pass.

Using methods described by Theis, Brown, and Meyer (1963) and applied by Luzier and Burt (1974), an analysis of the specific capacity of more than 100 wells for which such data were available indicated an average transmissivity of approximately $0.1 \text{ ft}^2/\text{s}$ for the primary aquifer system. Development of the transmissivity value applicable to each cell involved adjusting this average value where necessary to obtain a match between computed and observed heads. The distribution of transmissivity resulting from this process is shown in figure 7.

The effects of structural dislocation (as discussed on p. 5), are shown clearly by the extremely low transmissivities ($<0.01 \text{ ft}^2/\text{s}$) along the Horse Heaven Hills escarpment. In the central lowland (subarea 4 in fig. 3) transmissivities average about $0.085 \text{ ft}^2/\text{s}$, whereas in the relatively flat, undisturbed areas in the western and northwestern parts of the basin, transmissivities are the highest. However, at only a few nodes do they exceed $0.5 \text{ ft}^2/\text{s}$.

Upper and Lower Confining Layers

A confining layer serves as an insulator between aquifers. That is, the effects of head changes in one aquifer are damped for considerable periods of time by the storage characteristics and relatively lower hydraulic conductivity of a confining layer before the aquifer on one side of a confining layer "feels" any effect of change in head in the other aquifer. As heads in aquifers on either side of such a confining layer change, there is a rapid change in the rate of flux from or to the confining layer, but the storage characteristics of the confining layer prevent the rapid migration of a new gradient across the confining layer. If the storage capacity of the confining layer is negligibly small, the rate of gradient migration across the confining layer is very rapid, and the effects of changing head in one aquifer have a rapid effect on the flux entering or leaving the other aquifer.

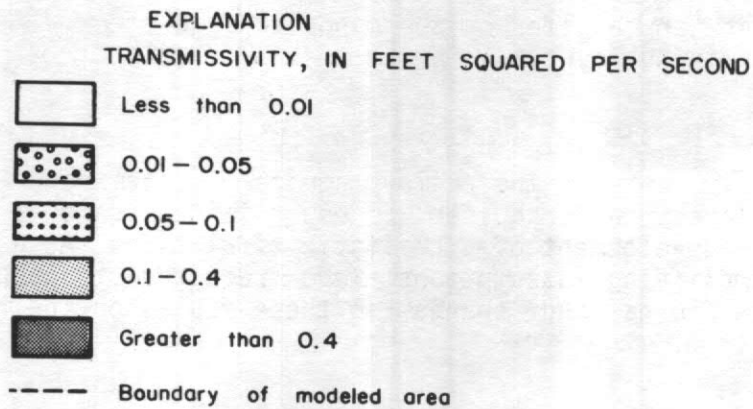
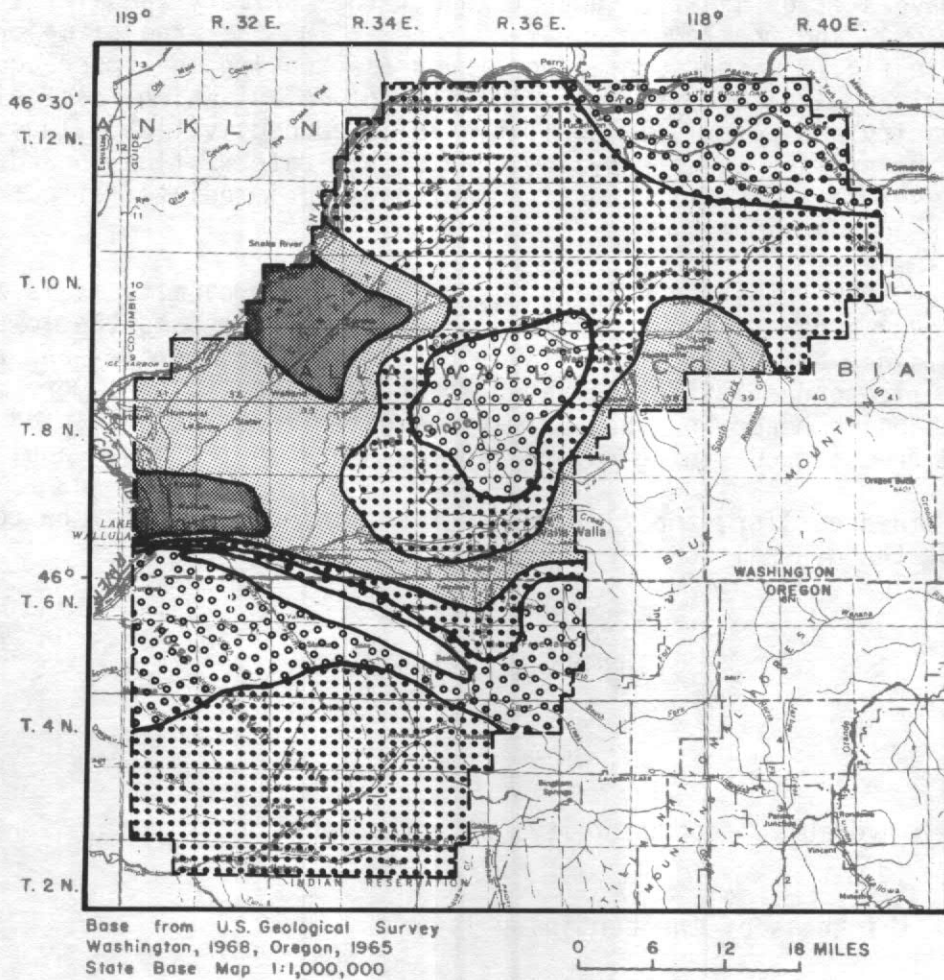


FIGURE 7.--Distribution of transmissivity in the digital-model area.

In the Walla Walla River basin, there are three aquifer zones, separated by confining layers (fig. 4)--the upper zone, the primary aquifer system (the modeled system), and the lower aquifer zone. In the area of major interest (subarea 4 in fig. 3), the confining layer separating the upper aquifer zone from the primary aquifer system is composed of clay which has significant storage capacity and relatively small hydraulic conductivities. Thus, changes in head in the primary aquifer system change the rate of flux to and from this confining layer to the primary aquifer, but have no immediate effect on heads in the upper aquifer zone.

Elsewhere, the upper confining layer is dense basalt, as is the entire confining layer separating the primary aquifer system and the lower aquifer zone. This dense basalt confining layer has negligible storage--and relatively large hydraulic conductivities compared to the clay confining layer. Thus, the effect of changing head in the primary aquifer zone has a "rapid" effect on flux to and from the confining layers, and on heads in the other aquifer zone.

As explained earlier, the flux across a confining layer may be computed by a formula of the general form:

$$\text{Flux} = \frac{K}{M} (h_p - h), \quad (4)$$

where

K = hydraulic conductivity of the confining layer,

M = thickness of the confining layer,

h_p = head in the modeled aquifer, and

h = head in an aquifer on the opposite side of the confining layer.

In simulating the flux between the primary aquifer system and the upper and lower confining layers and aquifer zones, limited data imposed severe restrictions on the development of a realistic simulation. As a result, many compromises and simplifying assumptions were required to approximate the effects of these fluxes and changes in these fluxes on the heads in the primary aquifer system.

The data limitation included:

1. No information on the K values for either upper or lower confining layers.
2. No information on thicknesses (M) of either confining layer, though in subarea 4 (fig. 3) this value might be approximated by the thickness of the clay unit described by Mac Nish, Myers, and Barker (1973, p. 8).
3. Sparse data on the primary aquifer zone outside subarea 4 (fig.3).
4. No data on heads in the lower aquifer zones, except in the southeastern part of subarea 4 and the adjacent western edge of subarea 5.

In the absence of real K and M values for use in equation 4 (p. 28) the K values for each confining layer were approximated by values from the literature for similar materials and were assumed constant for the area. M values were arbitrarily set, assuming a uniform thickness for the upper and lower confining layers except in subarea 4 (fig. 3), where the apparent thickness of the clay (Newcomb, 1965, p. 13A) was used as the initial trial value in the modeling procedure. As these values were either estimated or interpreted they were subject to frequent modification in the calibration of the model--this aspect is addressed further in the discussion of the steady-state model (p. 34).

Owing to the sparseness of data on heads in the lower aquifer zone, the head distribution for the model was developed in the following manner:

Water levels in the lower aquifer zone are best defined in the southeastern part of subarea 4 and the western edge of subarea 5 (fig. 3) as several wells in this area tap the lower aquifer. Farther to the west, however, few wells tap this aquifer zone, and west of Lowden and north of Dry Creek only one or two wells (table 1; wells in section E of fig. 4) have water levels strongly influenced by the head in the lower aquifer. The distribution of data suggests that the head difference between the primary aquifer system and the lower zone is about 100 feet along the eastern margin of subarea 4 and approaches zero within about 14 miles to the west. The head distribution in the lower aquifer was then constructed by assuming that this difference in gradient occurred in a 14-mile-wide zone skirting the Blue Mountains.

To evaluate this multilayer aquifer system, the flux between the primary aquifer system and lower aquifers across the confining layer would be more properly treated by a multilayer model, as changes in head in the lower zone have a rapid effect on the head in the primary aquifer system. However, this would require that the flux across the confining layer be computed because the heads in both aquifers are changing in response to stress.

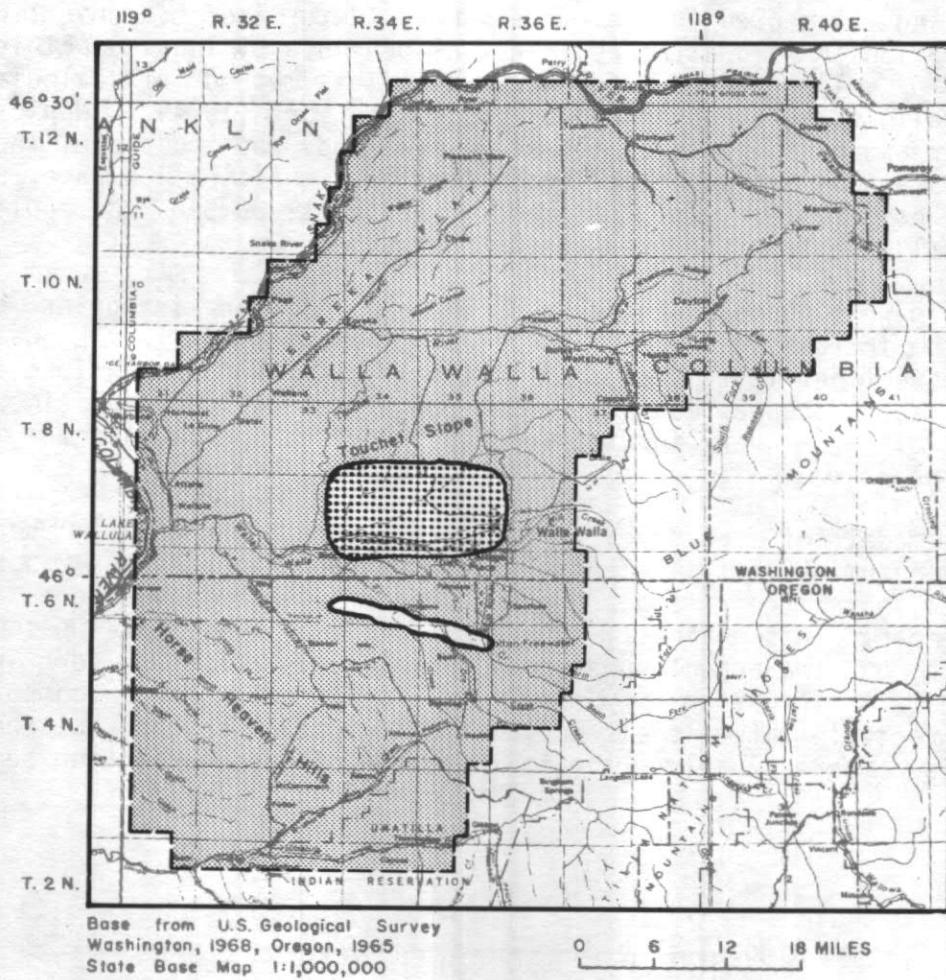
In view of the lack of reliable data for K and M in the confining layers, and the sparse head data for the lower aquifer and parts of the primary aquifer system, a single-layer model was used. This required that some simplifying assumption be made to accommodate the expected K and M differences existing between the upper and lower confining layers in subarea 4.

Basically, the assumption made for the upper confining layer was that, regardless of head changes in the primary aquifer system, the steady-state flux would be maintained. While the assumption is technically invalid, the insulating effect of this confining layer prevented the changing head in the primary aquifer from affecting heads in the upper aquifer. The result is that, while the flux between the confining layer and the principal aquifer system changes rapidly in response to cyclic irrigation pumpage, the amount of flux is so small that it does not seriously affect heads in the principal aquifer zone. (The effects are discussed further in a discussion of response to stress on page 39.) The lower confining layer required different treatment in that this layer has negligible storage and the effects of head change in the primary aquifer have a rapid effect on heads in the lower aquifer zone. To approximate the effects of this rapid response of the lower aquifer zone, the head in the lower aquifer is adjusted between time steps, the adjustment being 45 percent of the change of head in the primary aquifer system on the previous time step. This empirical approximation of the rate of water-level decline in the lower aquifer is not a rigorous treatment of the hydraulic realities, but it does permit an approximation of the effects that historic head changes in the lower aquifer have had on the heads in the primary aquifer--and the rate of flux from that aquifer. This adjustment introduces a lag of one time step in the heads computed for the lower aquifer, and it results in some error in the computation of flux between the aquifers. However, this error is minimized by choosing time-step lengths such that only small amounts of drawdown in the primary aquifer system occur during any time step. This error is further discussed under the description of the transient model (p. 37).

All assumptions, simplifications, and compromises regarding vertical fluxes between the primary aquifer system and aquifer zones above and below introduce errors in the digital model, some of which may be compensating. It must be emphasized, however, that, in spite of the assumptions and compromises made, the simulation model has reasonably reproduced the effects of 72 years of pumpage in subarea 4.

Storage Coefficient

Price (1960, p. 29) reported a storage coefficient of "about 0.0002" from an aquifer test in the city of Walla Walla. Such an extremely low storage coefficient is to be expected from the tremendous structural rigidity of the basalt and from the fact that the primary aquifer system is confined by beds of low hydraulic conductivity. La Sala and Doty (1971, p. 35) reported that storage coefficients in aquifers in basalt of the Columbia River Group in the Hanford area ranged from 0.0006 to an incredibly low value of 0.0000014. For a basalt aquifer zone at a depth of 362-412 feet, comparable to that of the primary aquifer system, La Sala and Doty reported a storage coefficient of 0.000066. In the Walla Walla study area, the values and geographic distribution of storage coefficients developed during calibration of the transient model showed that a value of 0.0002 was too low to account for the observed annual amplitude of the well hydrographs, and an average value of 0.00047, with larger and smaller values in some areas, gave the best overall fit. The distribution of storage-coefficient values used in the digital model is shown in figure 8.



EXPLANATION

Storage coefficient

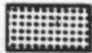

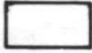

	0.00009
	0.00047
	0.00475
	Boundary of modeled area

FIGURE 8.--Distribution of storage coefficients within the digital-model area.

Pumpage

The pumping rates used in the model were determined by converting annual power consumption in kilowatthours (kWh), as provided by local electrical power companies, to volume rates of withdrawal. This method of calculation of pumpage parallels that described by Luzier and Burt (1974). Municipalities pump the year around in parts of the study area and, when possible, the overall pumpage computations were checked against metered municipal pumpage, and these were found comparable. In the model, municipal pumpage was applied as an average annual stress in the areas of withdrawal.

Irrigation-well pumps are turned on and off on irregular schedules throughout the irrigation season. These abrupt changes in withdrawal produce dramatic fluctuations in the rates of vertical flux ("W" in equations 1 and 2). To simulate such changes during a model run, excessive computer time would be needed to permit the very short time steps required to simulate the irregular pumping stress.

In the model of the primary aquifer system, irrigation pumping was simulated by assuming that all irrigation pumps were turned on in March and that they withdraw their total computed annual pumpage at a constant rate through November. This obviously is a simplification that contains some error, as is shown by the annual power-consumption curve (fig. 9) for irrigation pumps. The simplification may result in a difference between computed water levels and actual water levels during the irrigation season, but these water levels should compare closely prior to the start of each irrigation season.

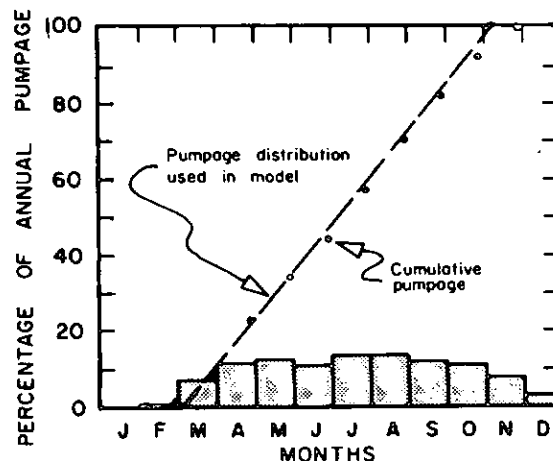


FIGURE 9.--Monthly distribution in 1969, of electric-power demand for irrigation, as reported by Columbia Rural Electric Association (written commun., 1970).

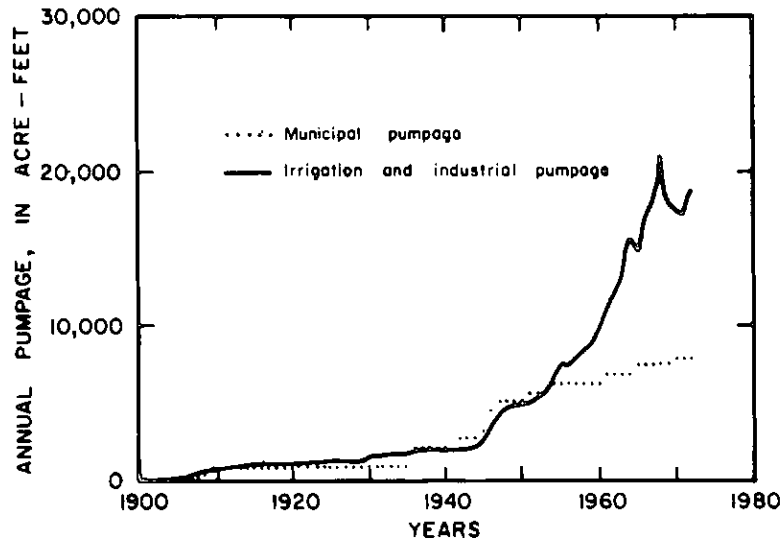


FIGURE 10.--Annual pumpage from the primary basalt aquifer system.

The 72-year history of pumping (1900-72) was reconstructed as follows:

1. For each irrigation well, the total kWh consumption during the year 1969 was obtained from power company records.
2. The 1969 computed pumpage from each well was assumed to approximate the annual average pumpage from that well in any year subsequent to the well's emplacement.
3. The annual pumpage during each year (1900 to 1972) was compiled by cumulating the average annual pumpage from each well in service during that year.
4. From 1948 to 1972 the major power company in the area kept records of the total kWh they supplied for irrigation pumps. Using the ratio of total 1969 pumpage to kWh consumption during 1969, an annual pumpage curve was constructed from 1948 to 1972, based on the total kWh used for irrigation in each of those years. Comparison of this curve with the equivalent segments of the curves developed in steps 1 to 3 above, showed a very close fit. As a further refinement, however, the percentage difference between the power-consumption curve and the accumulated pumpage curve was applied to the annual average pumpage from individual wells for each year (1948-72).

The results of this procedure generated the annual pumpage from the primary aquifer system for the model, as depicted in figure 10.

Municipal pumpage was calculated by the same process used to compute irrigation pumpage, except that no adjustment based on the irrigation-power curve was made. The pumpage distribution thus derived appeared to be reasonable for modeling purposes. The method of calculation used for the model showed a total pumpage from the basalt of 1,200 acre-feet during the year 1958; this compares favorably with the estimate of 14,800 acre-feet for that same year reported by Newcomb (1965, p. 61).

Aquifer Boundaries

Perhaps the most important compromises in model design are those made at the boundaries of the model. Figure 4 shows how ground water is discharged along the Snake and Columbia Rivers. Note that the actual no-flow boundary for each aquifer zone occurs in a different position. These no-flow boundaries, at least in the primary aquifer system and the lower aquifer zone, are to the north and (or) west of the rivers, owing to the substantial recharge from the vicinity of the Blue Mountains and the absence of comparable recharge in areas to the north and west of the two rivers. However, in the digital model the rivers are used as the boundary for all aquifer zones.

In simulation, a constant-head boundary was employed to maintain discharge from the primary aquifer system. As long as neither the pumping nor the elevated river levels behind dams strongly affects the gradient in the primary aquifer system at this discharge boundary, the constant-head approximation will simulate the actual conditions with reasonable accuracy.

Employing similar reasoning, a simplifying approximation of a constant-gradient boundary was employed along the recharge boundary flanking the Blue Mountains. This was necessary because the distribution of heads in the basalt-aquifer system in the Blue Mountains is not known. This simulated condition maintains the inflow from the Blue Mountains as a constant, although in the real system some steepening of gradients in this area undoubtedly occurs and the flux increases somewhat over that of the steady-state conditions.

In the actual hydrologic system, the northeastern and southern boundaries (extending between the Blue Mountains and the Snake and Columbia Rivers) are no-flow boundaries, because the boundaries parallel flow lines in the aquifer. It was expedient, however, to regard these areas as constant-head boundaries because the effects of hydraulic stress in the model are not strongly felt at these boundaries, and changes in the net rates of flux to and from these boundaries are very small.

Steady-State Model

The steady-state model simulates the primary aquifer system prior to the artificial stress imposed by man.

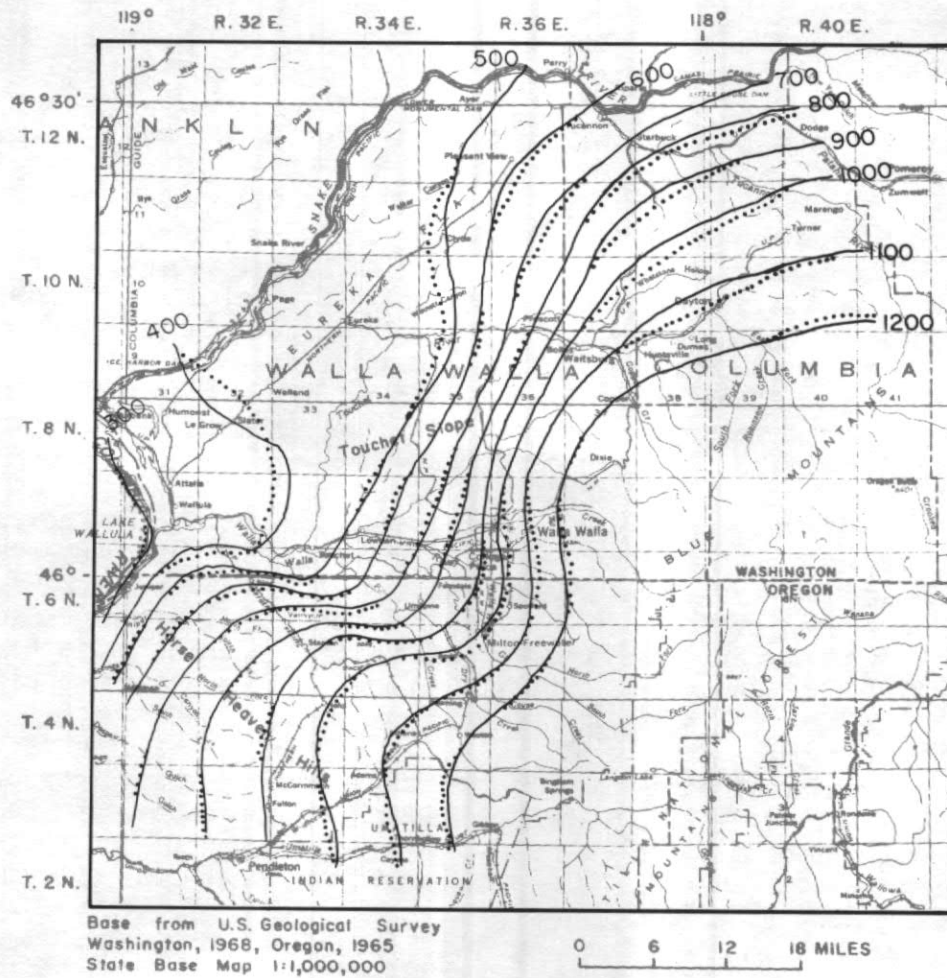
For calibration, known and estimated parameters and boundary conditions were entered into the model and adjustments were made in certain parameters until an acceptable match was obtained between observed heads and heads computed by the digital model. (All estimated values are subject to adjustment within reasonable limits.) The process began by adjusting transmissivity values in the primary aquifer system--subsequent adjustments to the thicknesses (M) and the conductivities (K) of the upper and lower confining layers were also necessary. The procedure of adjustment is basically a trial-and-error process, within constraints imposed by the known values of head, estimated

transmissivities, and the gross water budget of the system. The results are shown in figure 11. In the area of greatest data density (the central lowland of the study area) the computed heads were generally within 10 feet, while for more than 85 percent of the modeled area the match was within 15 feet of the observed heads. Two areas in which the match was relatively poor (more than 20 ft variance) were in the Horse Heaven Hills, and in the north-central part of the modeled area, paralleling the Touchet River valley west of Waitsburg; the maximum error here was 43 feet. North of the Touchet River, observed head data were so sparse that extensive adjustment of estimated model values was not considered practical.

The water budget for the digital model under the steady-state condition showed 114,000 acre-feet per year entering the model laterally from the Blue Mountains, with an additional 18,000 acre-feet per year entering from overlying basalt aquifers in the Horse Heaven Hills. The total of 132,000 acre-feet per year of recharge to the primary system is considered to be derived mostly from precipitation on the Blue Mountains. Outflow from the system ultimately reaches the Snake and Columbia Rivers and, under the steady-state simulation, equaled the inflow of 132,000 acre-feet per year.

Within the model, the discharge is subdivided into the components of lateral and vertical discharge near the two river systems (97,500 acre-ft/year) and discharge to the rivers via adjacent aquifer zones (34,500 acre-ft/year) in the interior areas of the model. The model shows that water is discharged laterally to the constant-head boundary at the Snake and Columbia Rivers at a rate of about 70,000 acre-feet per year. In reality the primary aquifer system is below these rivers and is not in good hydraulic connection with them. As discussed earlier, the discharge from the primary aquifer system is vertically upward over a broad region near the rivers and extends perhaps tens of miles on either side of the rivers. Thus, the results of the model must be viewed in the light that the model simulates reasonably well boundary conditions for the central lowland area (that is, the developed area), and does not simulate the actual condition at the boundary.

Owing to lack of sufficient head data in the discharge area, little effort was spent balancing the discharge of the primary aquifer system between vertical upward discharge, which should be the largest, and lateral flow past the Snake and Columbia Rivers to the apparent line sink some distance to the north and west. (See fig. 4 for the primary aquifer system.) In addition, water lost to the deeper zones farther east in the basin, though included in the 34,500 acre-feet per year discharge, was not simulated as returning to the discharge area. Water which enters the deeper zones in the Blue Mountains, to the east of the arbitrary model boundary, was neither simulated as entering the circulation in the discharge area nor accounted for in any budget; the total quantity is probably less than 20,000 acre-feet per year. If needs develop for further precision in simulating flow conditions near the discharge boundary, these factors would have to be evaluated.



EXPLANATION

- 900 — Reconstructed WATER-LEVEL CON-
TOUR - Shows altitude of water level.
Contour interval 100 feet. Datum
is mean sea level
- Computed water levels

FIGURE 11.--Comparison of water-level contours in the primary basalt aquifer system in 1900 with water-level contours computed by the digital simulation model.

Transient Model

The transient model used the solution of the steady-state simulation for initial conditions. In the conversion, several minor adjustments were made in values of input data used in the steady-state model in order to permit use of the computed steady-state heads in the transient model. This was necessary because, if the original observed head data had been used, the transient model would have had to run for some period of time to achieve the steady-state solution before the application of pumping stress. The conversion is limited to two input data sets whose values were originally estimated--namely the effective thickness of the upper and lower confining layers. The values of effective thickness in each cell were adjusted so that, under the heads computed in the steady-state solution, the same fluxes from the upper and lower confining layers would occur as under the initial, observed head condition in the primary aquifer system. For most cells, the changes were less than 10 percent of the original estimated values.

Calibration of the transient model was accomplished by adjusting two components of the model which were constant under steady-state conditions. The storage coefficient was changed from the initial zero value to an average value of 0.00047 and then adjusted, primarily to obtain the proper amplitude of annual fluctuations in the water levels. The other adjustment was to the rate of decline of the head in the lower aquifer zone with respect to the primary aquifer system.

As explained earlier in the discussion of the upper and lower confining layers, the adjustment of heads in the lower aquifer zone is empirical and is based on the head change in the primary aquifer system. This places some restrictions on the the time-step structures. In order to maintain stability in the solution of flux values between the primary aquifer system and lower aquifer, the adjustments of heads in the lower aquifer should be made frequently during periods of rapid head change in the primary aquifer system. When a new stress condition imposed on the simulation model causes rapid changes in water levels, the time step incrementation is reset to the first time step shown in table 2. Such a stress change occurs at the beginning and end of an irrigation pumping season. As the aquifer responds to the new stress, rapidly at first and more gradually as time passes, the time steps become larger. The time step length increases by a factor of 3 for the first three time steps, and by a factor of 1.5 thereafter. If no new stress conditions are imposed the time-step length can increase indefinitely. This time-step structure resulted in a readjustment of the flux to the lower aquifer zone for small (generally less than 7 ft) increments of drawdown change in the primary aquifer system.

TABLE 2.--Time-step equivalents of real time from the beginning or cessation of irrigation pumping

Time steps	Duration	Elapsed time from start (approximate)
1	1.0×10^5 seconds	1.2 days
2	3.0×10^5 seconds	3.6 days
3	9.0×10^5 seconds	14 days
4	13.5×10^5 seconds	29 days
5	20.2×10^5 seconds	52 days
6	30.4×10^5 seconds	87 days
7	45.6×10^5 seconds	140 days
8	68.3×10^5 seconds	219 days
9	103×10^5 seconds	338 days
10	154×10^5 seconds	1 yr 151 days
11	231×10^5 seconds	2 yr 53 days
12	346×10^5 seconds	3 yr 88 days
13	519×10^5 seconds	4 yr 325 days
14	778×10^5 seconds	7 yr 128 days
15	1170×10^5 seconds	11 yr 146 days

The model is designed to run for stress periods of varying lengths. The time-step sequence starts when the stress condition is imposed and progresses according to the schedule in table 2 until the time-step increment being used exceeds the end of the stress period. The model then reduces the final time-step increment to coincide with the end of the stress period and returns to time step 1 for the following period. For example, if an irrigation season is specified as beginning March 13 and ending November 4 (236 days), 9 time steps are required, but the model reduces the 9th time step to 14.1×10^5 seconds; thus, the total elapsed time is 236 days. The following nonirrigation season would be 129 days long. Table 2 shows that 7 time steps would be required to reach that total elapsed time, with the model truncating the 7th time step to 36.3×10^5 seconds to come out exactly 129 days. Thus, a complete annual cycle will require 16 time steps, 9 for the irrigation season, and 7 for the nonirrigation season.

Observed and Calculated Response to Stress

The value of the transient model may be measured by the precision with which it can reproduce the actual effects of future stress. There are two ways of evaluating the probability of the model's capability to reproduce future stress effects: (1) compare the January 1972 observed and computed distribution of water levels, and (2) compare actual annual hydrographs for specific wells tapping the primary aquifer system to those generated by the model.

The predicted head distribution after 72 years of pumping is shown in figure 12. The data from which this figure was prepared were generated by the transient model. As shown in figures 2 and 12, the general directions of flow in the primary aquifer system have not changed significantly since pumping began. However, significant steepening of head gradients associated with some local changes in direction of flow has occurred in places within the central lowland (subarea 4), where heavy pumping has produced water-level declines of as much as 130 feet.

Plate 1 (in pocket) shows the water-level contour map based on model-generated data in the developed area. Water-level measurements in basalt wells tapping the primary aquifer system are shown for comparison. Water levels from other wells tapping (in part) upper and lower aquifer zones are also shown, and are indicated as being influenced by heads in upper or lower aquifer zones.

Figures 13 to 15 show the annual hydrographs of several wells located within the developed area that tap the primary aquifer system. The amplitude of the computed hydrographs is somewhat larger than that of the observed data. This is most likely due to the effect of leakage to and from the clay layer in subarea 4 and could be modified by enlarging the storage coefficient.

During the irrigation pumping season, when water levels are being lowered, water stored in the confining clay layers moves into the aquifer. During the nonirrigation season, when water levels rise, water moves back into the confining layers. The effect of this process in the natural system is to dampen the amplitude of annual water-level fluctuations. The digital model does not simulate this "transient leakage" phenomena and, to compensate, the model value of the storage coefficient has been made larger than the storage coefficient of the real aquifer. Because the assigned storage coefficient is higher than the actual storage coefficient, further adjustments in other input parameters, to provide for closer simulation of water-level fluctuations, was considered to be unjustified.

By 1972 the fluxes to and from the primary aquifer system had changed from their initial year-1900 values. A comparison of water budgets for 1900 and 1972 as computed by the digital model is shown in table 3.

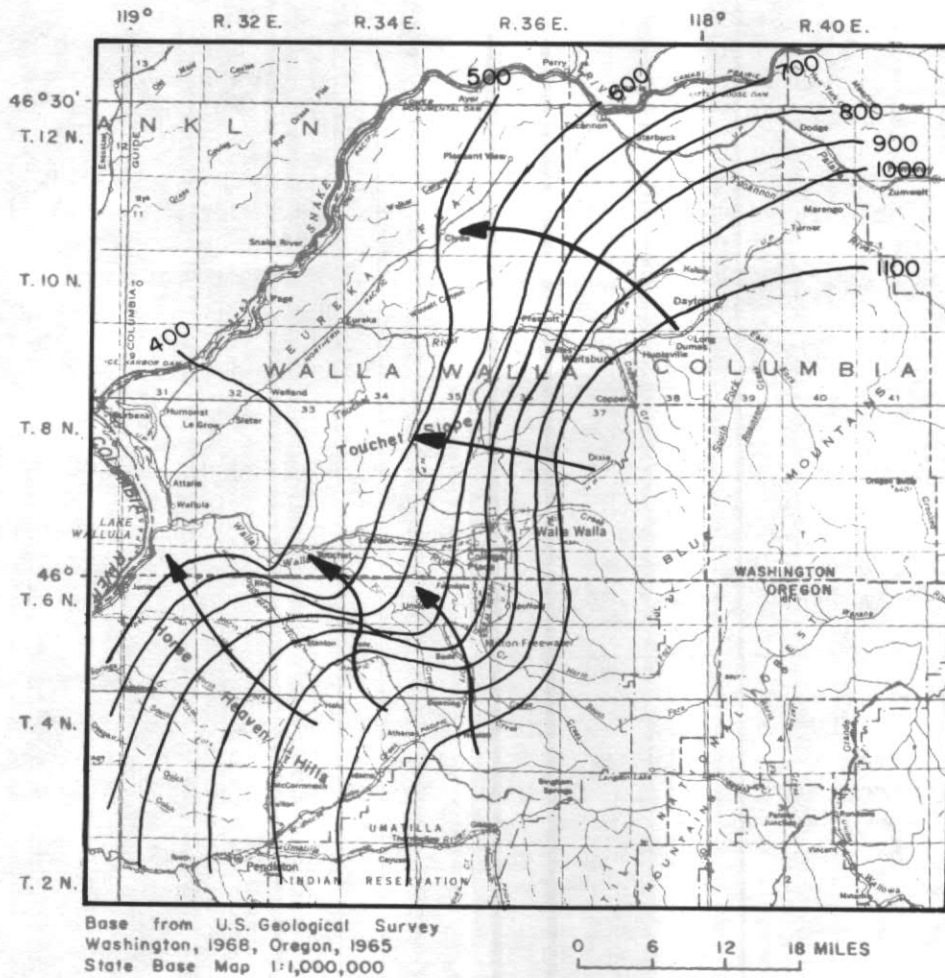
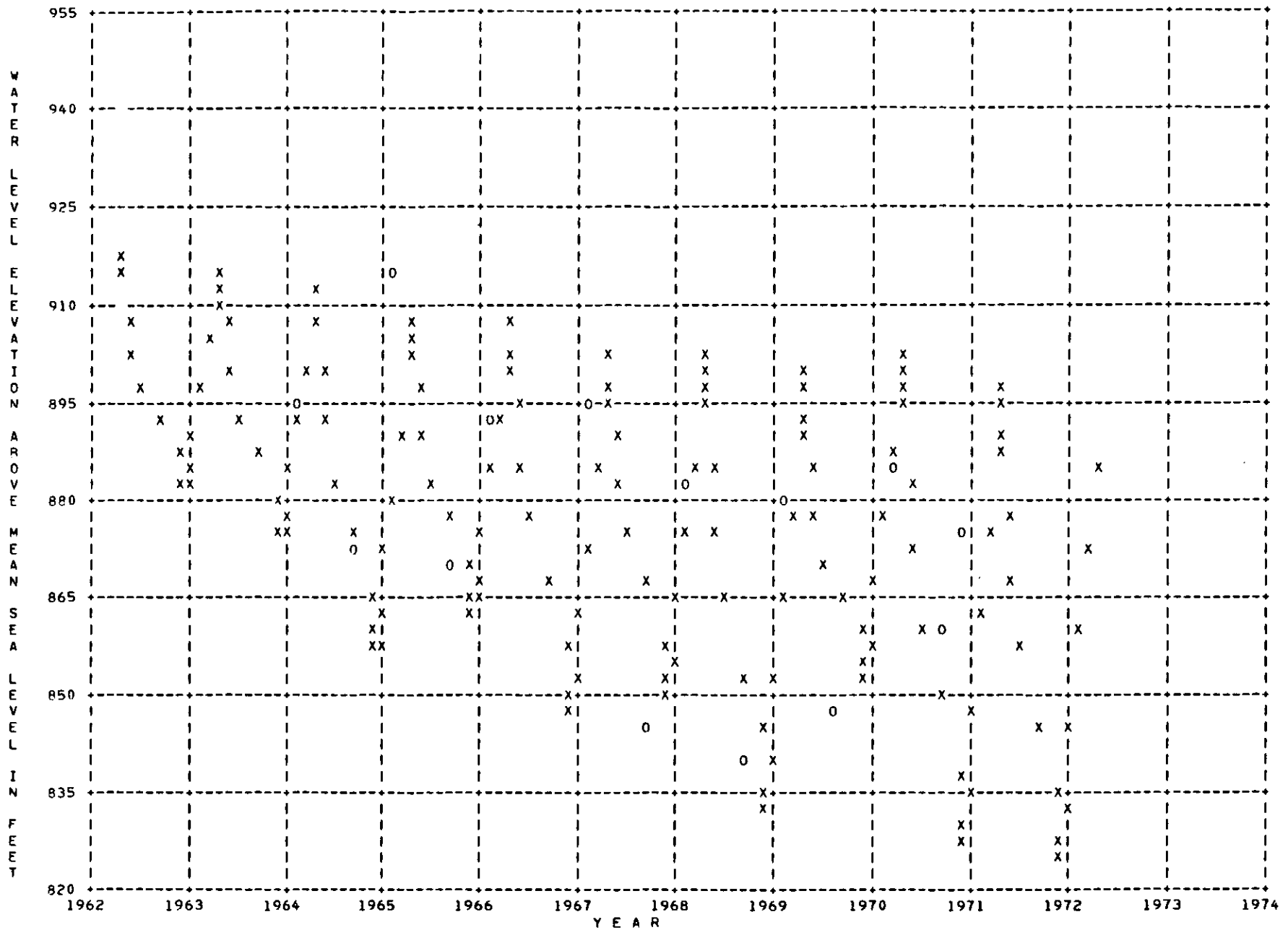


FIGURE 12.--1972 water-level contours, as predicted by the digital model. Arrows indicate general direction of ground-water movement.



DIGITAL MODEL

FIGURE 13.--Comparison of observed water levels (O) in well 07N/36E-17L1 with computed water levels (X) in node 20,22 of the digital simulation model of the primary basalt aquifer system.

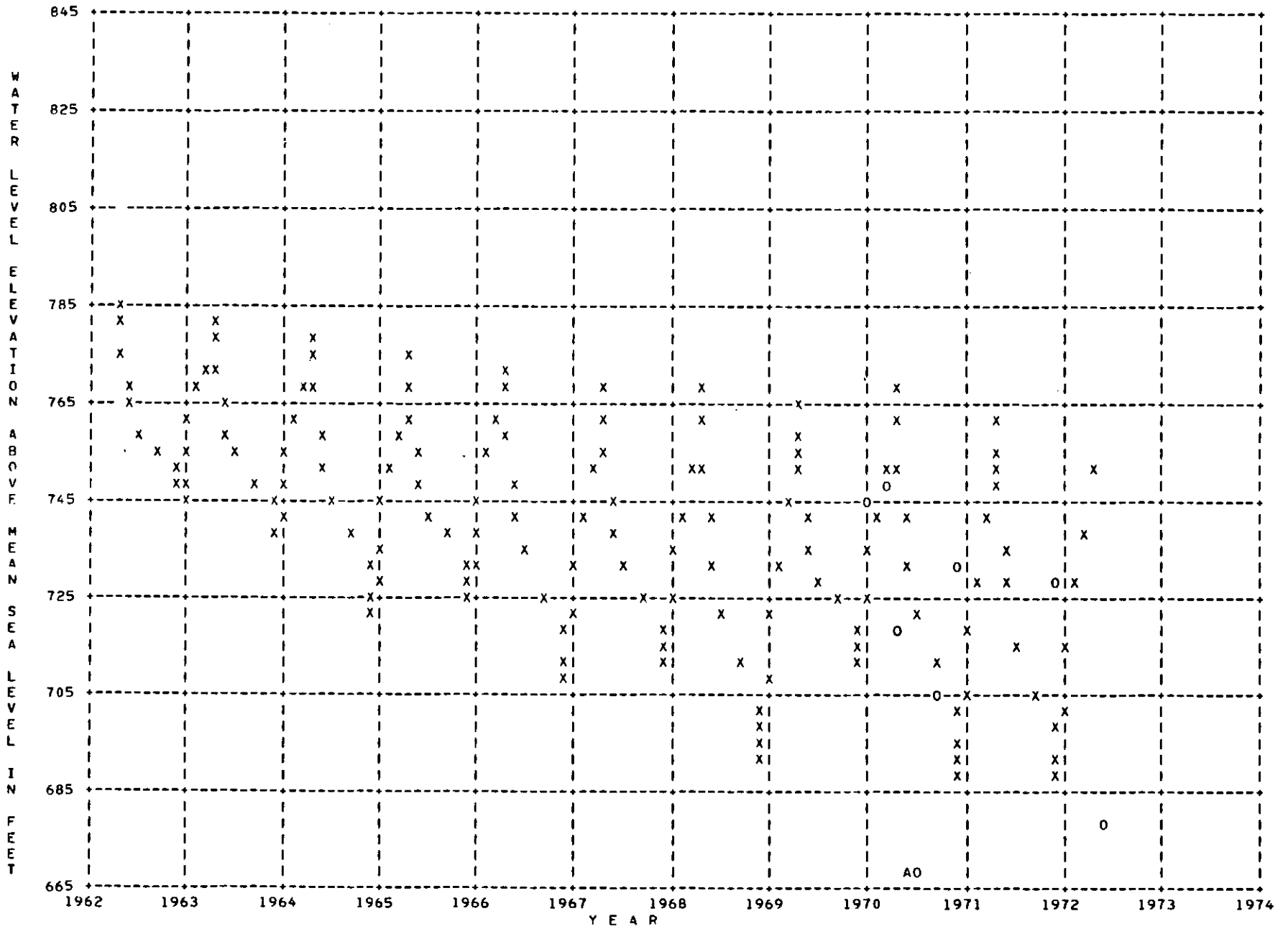


FIGURE 14.--Comparison of observed water levels (O) in well 07N/35E-35A1 with computed water levels (X) in node 17,25 of the digital simulation model of the primary basalt aquifer system.

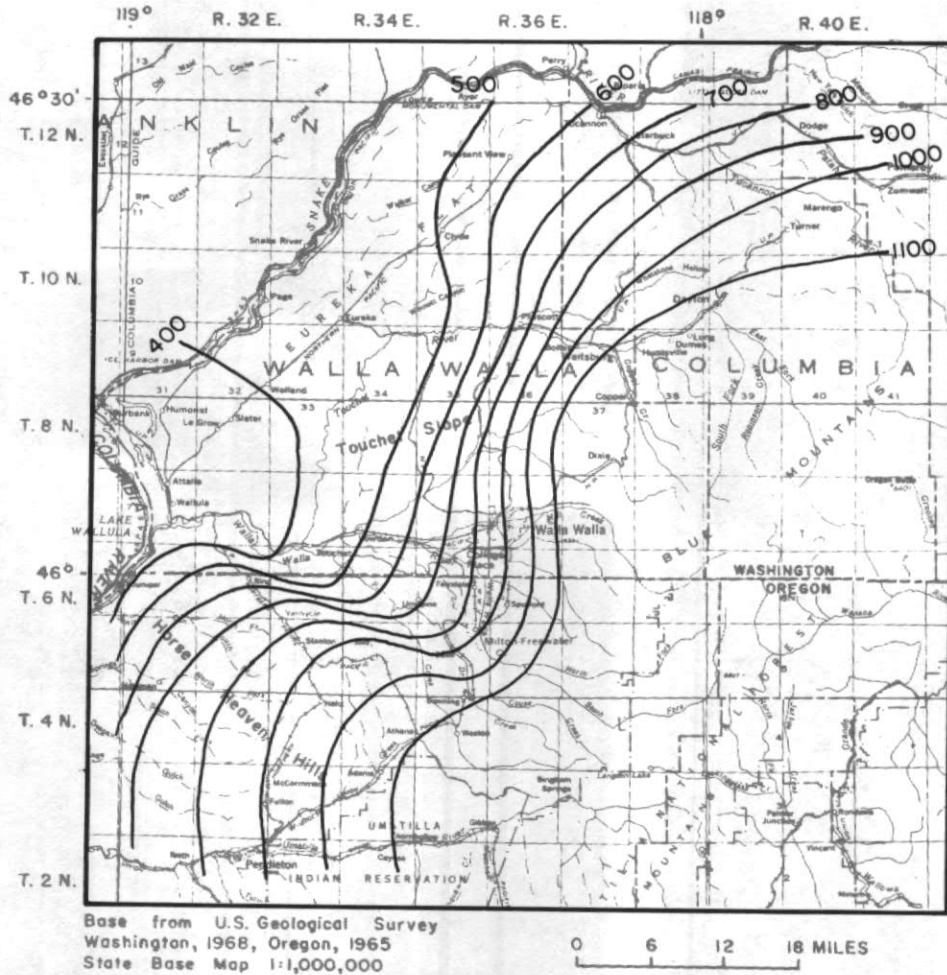
TABLE 3.--Water budgets for the study area in 1900 and 1972

	Acre-feet/yr	
	1900	1972
Inflow:		
From Blue Mountains and foothills-----	114,000	120,500
From Horse Heaven Hills-----	18,000	18,000
Change in storage-----	0	500
Outflow:		
To Columbia and Snake Rivers-----	97,500	89,000
To adjacent aquifers-----	34,500	22,000
To pumpage-----	0	28,000

Projection Based on 1972 Pumpage

The transient model was used to project the effects of continuing the 1972 pumping stress to 1980. Figure 16 shows the resultant water-level contours and figures 17-19 show the hydrographs of the three wells shown in figures 13-15. The hydrographs show that after about 3 years the heads should stabilize a few feet below the 1972 levels.

The manner in which pumpage was entered in the model permits a quick adjustment for changes in pumping stress. If the areal distribution of increases or decreases in pumping in a given year is similar to the areal distribution of the 1972 pumping, then the entire pumpage-data set may be adjusted up or down by the ratio of that year's irrigation power consumption to the power consumption in 1972.



EXPLANATION

— 500 — WATER-LEVEL CONTOUR — Shows altitude of water level. Contour interval 100 feet. Datum is mean sea level

FIGURE 16.--Water-level contours projected for 1980, from data computed in the digital model, and assuming continued pumping at the 1972 rate.

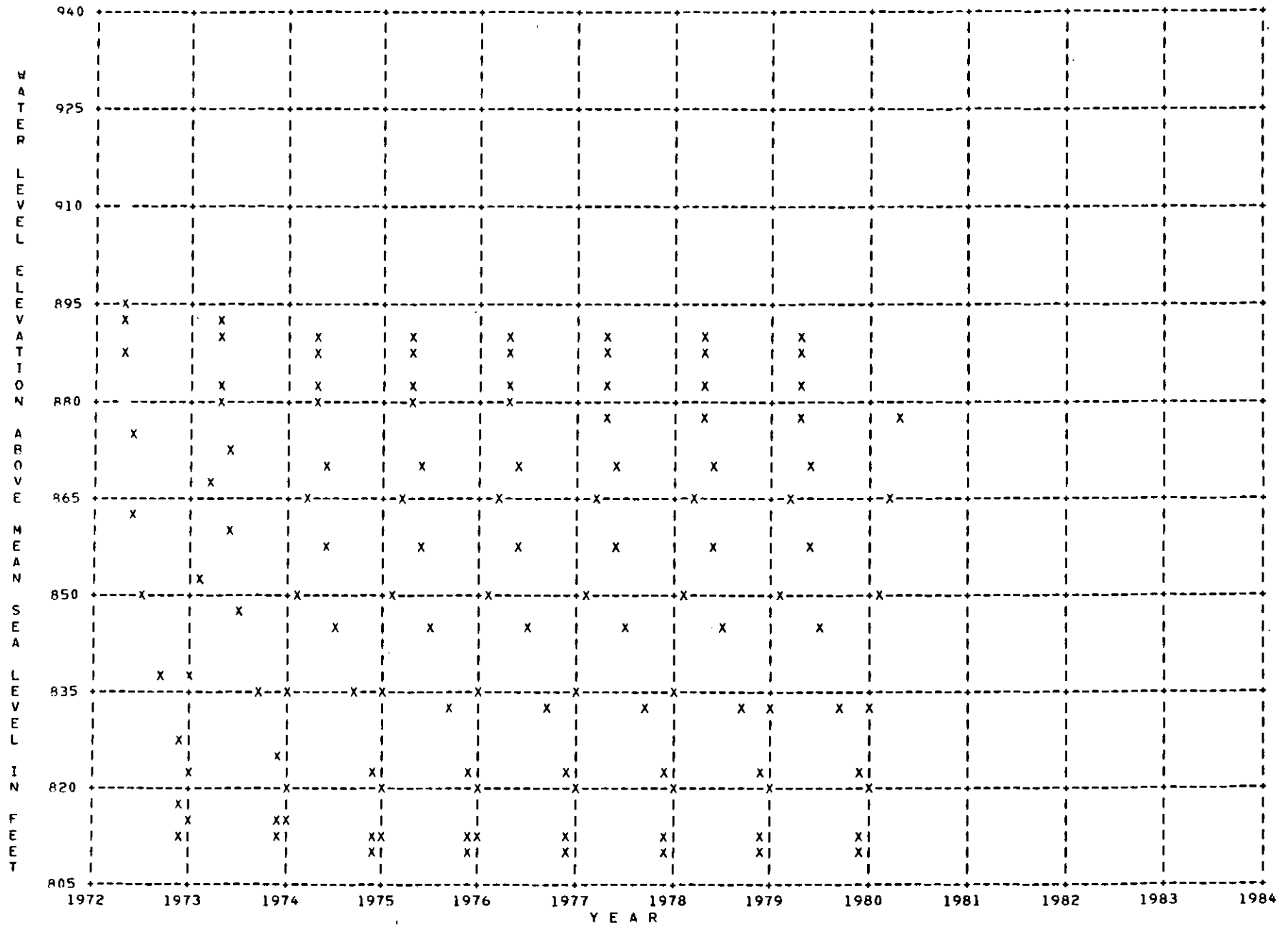
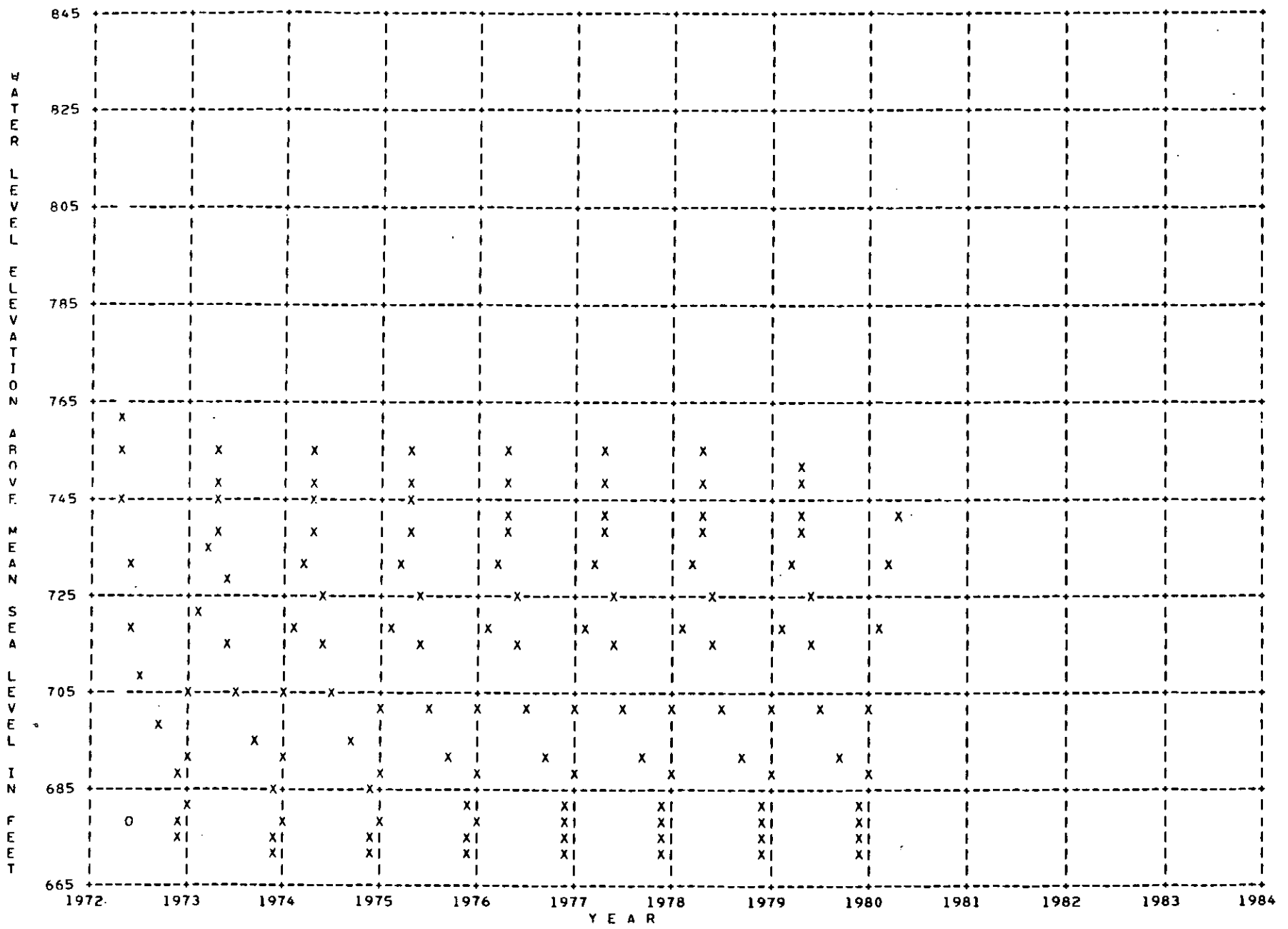


FIGURE 17.--Water levels computed to 1980 in well 07N/36E-17L1, in node 20,22 of the digital simulation model of the primary basalt aquifer system.



DIGITAL MODEL

FIGURE 18.--Water levels computed to 1980 in well 07N/35E-35A1, in node 17,25 of the digital simulation model of the primary basalt aquifer system.

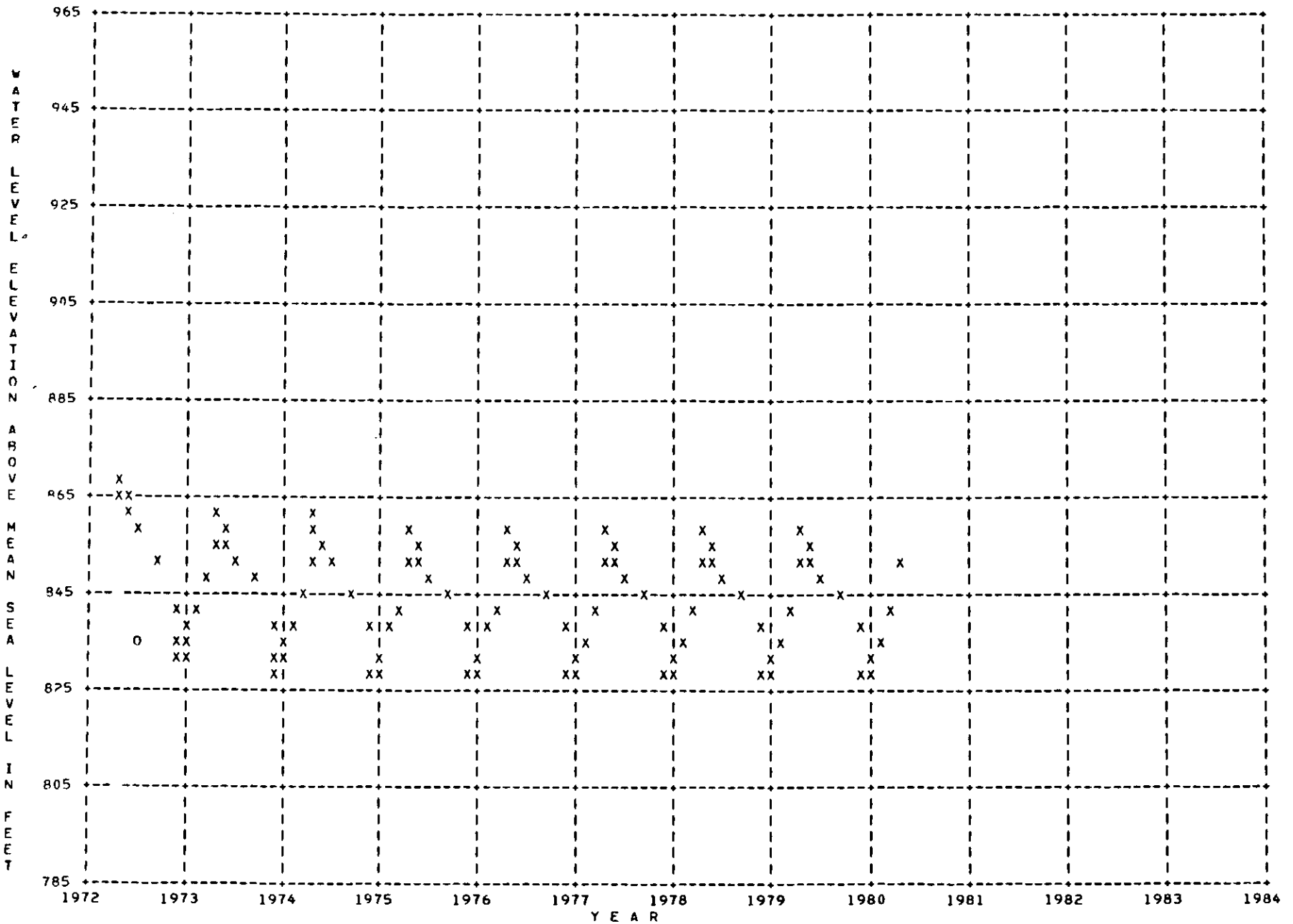


FIGURE 19.--Water levels computed to 1980 in well 05N/35E-12F2, in node 09,24 of the digital simulation model of the primary basalt aquifer system.

Limitations and Areas for Future Investigation

Within specified limits the digital model of the primary aquifer system in the study area could be used to simulate and evaluate the effects of present pumping stress, and to project the effect of future stress. Although the model was calibrated from data from a 72-year pumping period, the empirical nature of the simulation of head changes in the lower aquifer zones will cause the accuracy of predictions to decrease with time. Two other items not treated wholly satisfactorily in the model are vertical leakage to the upper zones and the changing flux of water entering the modeled area from the Blue Mountains. However, as a result of simplifications, compromises, and compensating errors in the simulation of these three facets, a reasonable approximation of the response of the real system to pumping stress appears to have been achieved.

At present, the model can evaluate with reasonable accuracy the effects of changing stresses and patterns of stress only in the presently developed subarea 4 (fig. 3). In other areas, the proximity to artificial boundaries (such as the Snake and Columbia Rivers and the Blue Mountains) and the empirical nature of the treatment of vertical fluxes will not allow great confidence in water-level projections based on future stresses which differ significantly from those of the present.

Additional data are needed to upgrade the digital model so that the effects of future stresses could be predicted with greater accuracy. The data most needed are the head relationships between the primary aquifer system and lower aquifer zones in all parts of the study area. In addition, data are needed that will provide for better definition of the head relationships between the primary aquifer system and upper aquifer zone in the discharge areas on both sides of the Snake and Columbia Rivers. With these data, and the available long pumping history for verification, the accuracy of the model in predicting the effects of stress could be increased. A further point of investigation might be the incorporation of the simulation of transient leakage from the overlying clay in subarea 4. However, this leakage is minor and for this reason was ignored in the present investigation.

In assessing the relative potential for further water development in the study area, the gravel aquifer (the upper aquifer zone in this report) described by Barker and Mac Nish (1976) offer a much greater potential for management and increased yield than does the primary aquifer system. The difference in the potential for management derives from the ability to manipulate both recharge and discharge in the gravel aquifer, whereas in the basalt only discharge can be manipulated effectively. Certainly, this should be a consideration when evaluating the priorities of further investigations in the Walla Walla River basin area.

REFERENCES CITED

- Barker, R. A., and Mac Nish, R. D., 1976, Digital model of the gravel aquifer, Walla Walla River basin, Washington and Oregon: Washington Dept. Ecology Water-Supply Bull. 45, 49 p.
- Bredehoeft, J. D., and Pinder, G. F., 1970, Application of the digital computer for aquifer evaluation: Water Resources Research, v. 6, no. 3, p. 883-888.
- Fenneman, N. M., 1931, Physiography of western United States: New York, McGraw-Hill Book Co., 534 p.
- Garrett, A. A., 1962, Artificial recharge of basalt aquifers, Walla Walla, Washington, in Geological Survey research, 1962: U.S. Geol. Survey Prof. Paper 450-C, p. C116-C117.
- La Sala, A. M., Jr., and Doty, G. C., 1971, Preliminary evaluation of hydrologic factors related to radioactive waste storage in basaltic rocks at the Hanford Reservation, Washington: U.S. Geol. Survey open-file report, 68 p.
- Luzier, J. E., and Burt, R. J., 1974, Hydrology of basalt aquifers and depletion of ground water in east-central Washington: Washington Dept. Ecology Water-Supply Bull. 33, 53 p.
- Mac Nish, R. D., Myers, D. A., and Barker, R. A., 1973, Appraisal of ground-water availability and management projection in Walla Walla River basin, Washington and Oregon: Washington Dept. Ecology Water-Supply Bull. 37, 25 p.
- Molenaar, Dee, 1968, A geohydrologic reconnaissance of northwestern Walla Walla County, Washington: Washington Dept. Water Resources Monograph 1, 1 pl.
- Newcomb, R. C., 1965, Geology and ground-water resources of the Walla Walla River basin, Washington-Oregon: Washington Div. Water Resources Water Supply Bull. 21, 151 p.
- Pinder, G. F., and Bredehoeft, J. D., 1968, Application of digital computer for aquifer evaluation: Water Resources Research, v. 4, no. 5, p. 1069-1093.
- Piper, A. M., Robinson, T. W., and Thomas, H. E., 1933, Ground water in the Walla Walla basin, Oregon-Washington: U.S. Geol. Survey open-file report, 99 p.

- Price, C. E., 1960, Artificial recharge of a well tapping basalt aquifers, Walla Walla area, Washington: Washington Div. Water Resources Water Supply Bull. 7, 50 p.
- 1961, Artificial recharge through a well tapping basalt aquifers, Walla Walla area, Washington: U.S. Geol. Survey Water-Supply Paper 1594-A, 33 p.
- Theis, C. V., Brown, R. H., and Meyer, R. R., 1963, Estimating the transmissibility of aquifers from the specific capacity of wells, in Bentall, Ray, compiler, Methods of determining permeability, transmissibility, and drawdown: U.S. Geol. Survey Water-Supply Paper 1536-I, p. 331-341.